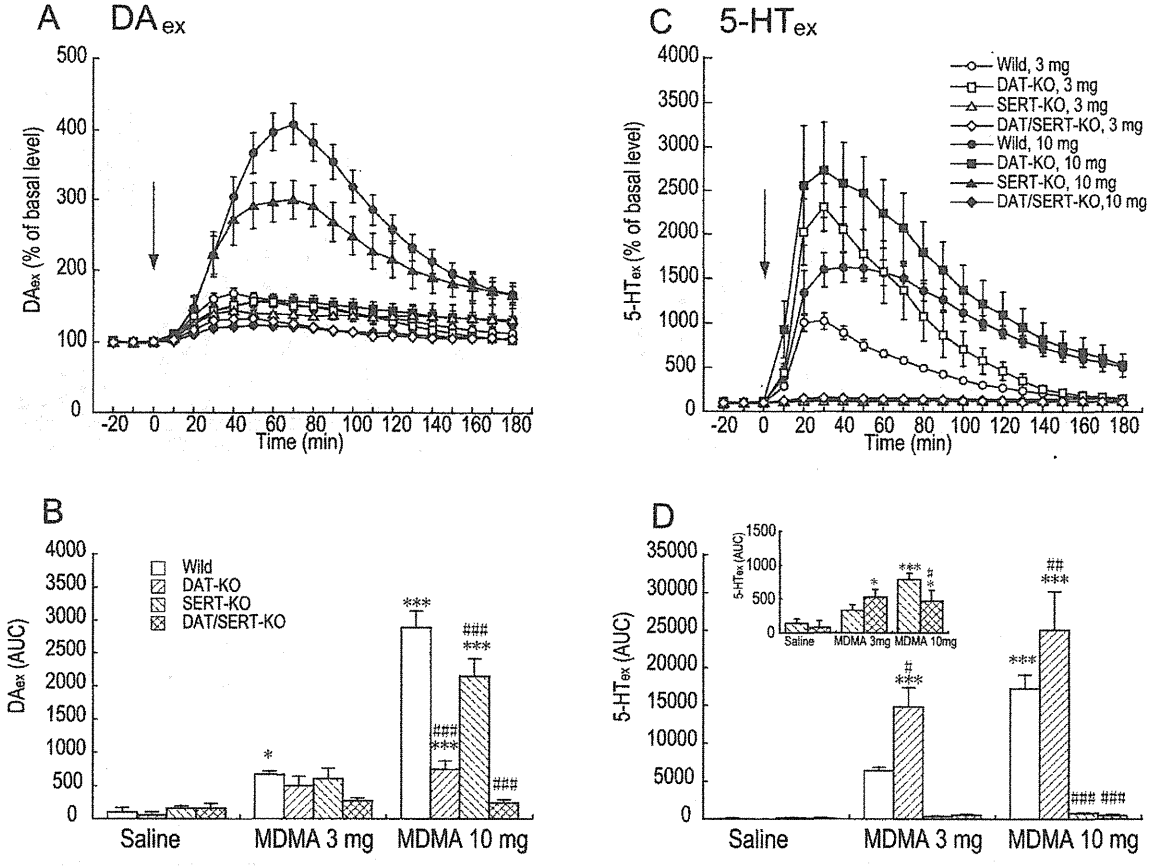

Fig. (1). Effects of MDMA on DA_{ex} and 5-HT_{ex} in the striatum in wildtype, DAT-KO, SERT-KO, and DAT/SERT double-KO mice. (A, C) Temporal pattern of DA_{ex} and 5-HT_{ex} before and after injection with saline or MDMA (3 and 10 mg/kg, s.c.). The arrows indicate drug injection time. Each point represents the mean ± SEM of the percentage of DA_{ex} or 5-HT_{ex} baselines. (B, D) Histogram representing the mean AUC (± SEM) of DA_{ex} or 5-HT_{ex} during the 180 min period after injection with saline or MDMA (n = 4-8). $^{*}p < 0.05$, $^{***}p < 0.001$, compared with saline group of the same genotype; $^{\#}p < 0.05$, $^{\#\#}p < 0.01$, $^{\#\#\#}p < 0.001$, compared with corresponding wildtype data in the same drug treatment (two-way ANOVA followed by Fisher's PLSD *post hoc* test).

MDMA (10 mg/kg) on 5-HT_{ex} in DAT/SERT double-KO mice was significantly less than in SERT-KO mice ($p < 0.05$; Fisher's PLSD *post hoc* test).

Effects of MDMA on DA_{ex} and 5-HT_{ex} in the PFC

MDMA (3 and 10 mg/kg) dose-dependently increased DA_{ex} in wildtype, DAT-KO, SERT-KO, and DAT/SERT double-KO mice (Fig. **2A, B**). Two-way ANOVA (drug × genotype) of DA_{ex} revealed a significant effect of drug ($F_{2,68} = 53.368$, $p < 0.001$) but no effect of genotype ($F_{3,68} = 0.203$, $p = 0.894$) and no drug × genotype interaction ($F_{6,68} = 0.408$, $p = 0.871$). MDMA (3 and 10 mg/kg) dose-dependently increased 5-HT_{ex} in wildtype and DAT-KO mice (Fig. **2C, D**). Two-way ANOVA (drug × genotype) of 5-HT_{ex} revealed significant effects of drug ($F_{2,68} = 32.357$, $p < 0.001$) and genotype ($F_{3,68} = 19.078$, $p < 0.001$) and a significant drug × genotype interaction ($F_{6,68} = 10.596$, $p < 0.001$). The effect of MDMA (10 mg/kg) on 5-HT_{ex} in DAT-KO mice was significantly less than in wildtype mice ($p < 0.01$; Fisher's PLSD *post hoc* test). When the effects of MDMA were analyzed only in SERT-KO and DAT/SERT double-KO mice, two-way ANOVA (drug × genotype) of 5-HT_{ex} revealed a significant effect of drug ($F_{2,29} = 28.906$, $p < 0.001$) but no significant effect of genotype ($F_{1,29} = 0.236$, $p = 0.631$) and no drug × genotype interaction ($F_{2,29} = 0.609$, p =0.551).

DISCUSSION

MDMA increased DA_{ex} and 5-HT_{ex} in the striatum and PFC, consistent with several previous microdialysis studies [7, 10-13]. In DAT/SERT double-KO mice, MDMA did not increase DA_{ex} in the striatum, and the increases in 5-HT_{ex} were minimal in the striatum and PFC. These results confirm that MDMA acts at both the DAT and SERT.

MDMA increased DA_{ex} in wildtype and SERT-KO mice, but not in DAT/SERT double-KO mice. In the absence of the DAT, MDMA-induced changes in DA_{ex} were smaller than in wildtype mice. Therefore, the DAT is likely mainly involved in the changes in DA_{ex} induced by MDMA. Although DAT-KO mice exhibited significant MDMA-induced increases in DA_{ex} levels, these increases were less than in wildtype mice. The increase in DA_{ex} produced by MDMA in DAT-KO mice may have two possible explanations. One possibility is that elevated 5-HT_{ex} levels produced by MDMA may influence DA release. Microdialysis studies have shown that MDMA, by increasing 5-HT_{ex}, indirectly increases DA_{ex} *via* an action at 5-HT_2 receptors [7, 8, 17]. Another possibility is that MDMA inhibits DA uptake into 5-HT axon terminals and increases DA_{ex}. The SERT is able to transport DA into 5-HT cells [26, 27], and the selective SERT blocker fluoxetine increases DA_{ex} in the striatum of DAT-KO mice [25].

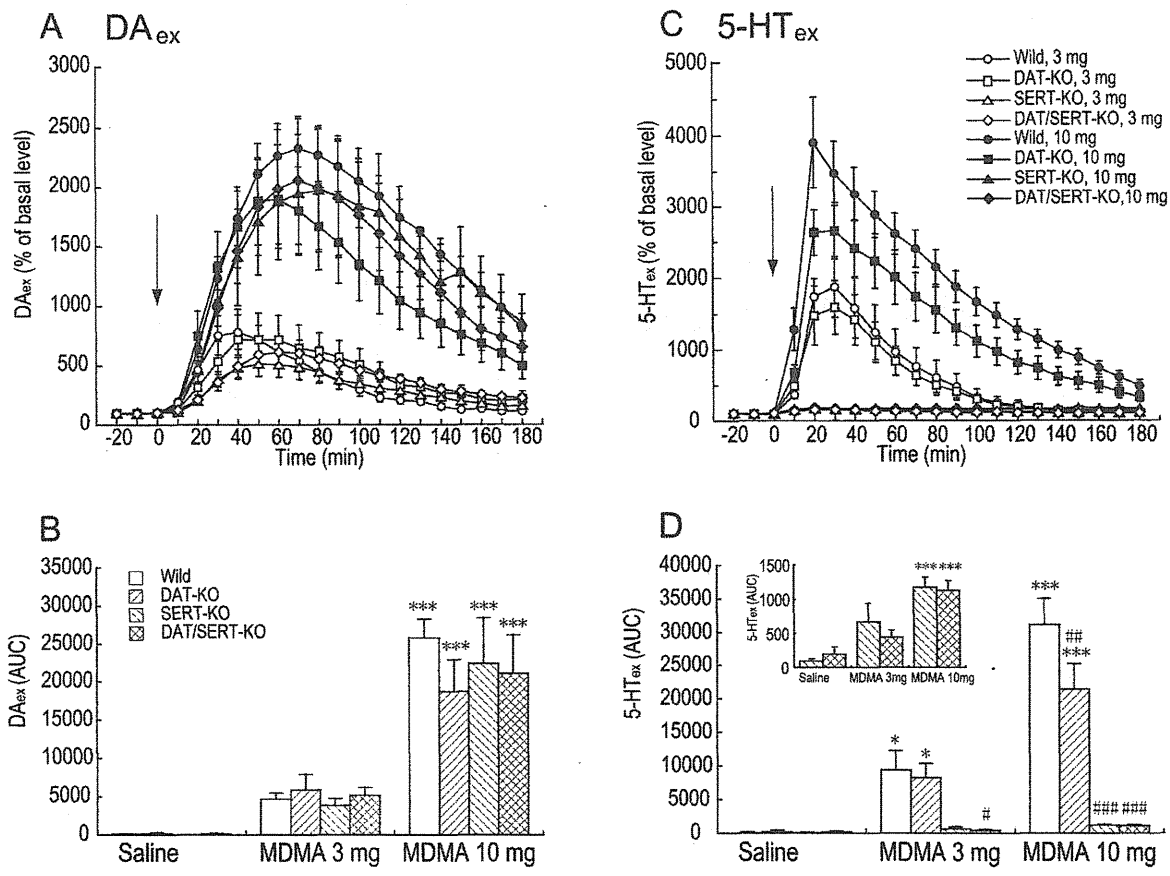

Fig. (2). Effects of MDMA on DA_{ex} and 5-HT_{ex} in the PFC in wildtype, DAT-KO, SERT-KO, and DAT/SERT double-KO mice. (A, C) Temporal pattern of DA_{ex} or 5-HT_{ex} before and after injection with saline or MDMA (3 and 10 mg/kg, s.c.). The arrows indicate drug injection time. Each point represents the mean ± SEM of the percentage of DA_{ex} or 5-HT_{ex} baselines. (B, D) Histogram representing the mean AUC (± SEM) of DA_{ex} or 5-HT_{ex} during the 180 min period after injection with saline or MDMA (n = 4-10). $^{*}p < 0.05$, $^{***}p < 0.001$, compared with saline group of the same genotype; $^{\#}p < 0.05$, $^{\#\#}p < 0.01$, $^{\#\#\#}p < 0.001$, compared with corresponding wildtype data in the same drug treatment (two-way ANOVA followed by Fisher's PLSD *post hoc* test).

Microdialysis studies have shown that NET inhibitors increased DA_{ex} in the PFC [28, 29], suggesting that NET can influence DA neurotransmission. Moron *et al.* (2002) reported that DA uptake in the PFC depends primarily on the NET [30]. This study showed a similar basal extracellular DA concentration in the PFC in DAT-KO and wildtype mice. DA_{ex} in the PFC is regulated by the NET. MDMA dose-dependently increased DA_{ex} in wildtype, DAT-KO, SERT-KO, and DAT/SERT double-KO mice. Therefore, MDMA may act at the NET and increase DA_{ex} levels in the PFC.

MDMA slightly increased 5-HT_{ex} in the striatum and PFC in mice lacking the SERT. The selective DAT blocker GBR12909 produced a substantial increase in dialysate 5-HT in SERT-KO mice that was not found in wildtype mice [25]. When the SERT is disrupted in SERT-KO mice, 5-HT is found in DA neurons in the substantia nigra and ventral tegmental area [31]. The DAT appears to play a compensatory role in 5-HT uptake in SERT-KO mice. Therefore, MDMA may act at the DAT and increase 5-HT_{ex} levels in the striatum in SERT-KO mice. The NET also appears to be able to play a role in 5-HT uptake [32]. In the PFC, MDMA may increase 5-HT_{ex} levels by acting at the NET in SERT-KO mice.

MDMA markedly increased 5-HT_{ex} in wildtype and DAT-KO mice. MDMA binds with higher affinity to the SERT than to the DAT [5, 6]. Consistent with *in vitro* results, MDMA produced greater elevations in 5-HT than DA. Relevant studies have shown that many of the subjective effects of MDMA in human volunteers are reduced after administration of a 5-HT_2 receptor antagonist or 5-HT reuptake inhibitors, suggesting that these effects are dependent on SERT-mediated enhancement of serotonergic transmission [33, 34].

In conclusion, the present microdialysis study using DAT- and/or SERT-KO mice demonstrated that MDMA targets monoamine transporters and stimulates predominantly serotonergic transmission.

ACKNOWLEDGEMENTS

We acknowledge Mr. Michael Arends for his assistance with editing the manuscript and Ms. Junko Hasegawa for her assistance with genotyping mice. This work was supported by a research grant (17025054) from the MEXT of Japan, by grants from the MHLW of Japan (H17-pharmaco-001, H19-iyaku-023, and 18A-3 and 19A-8 for Nervous and Mental Disorders), by a grant from the Smoking Research Founda-

tion, and by a grant from the Mitsubishi Foundation for Social Welfare Activities.

REFERENCES

[1] Johnson, M.P.; Conarty, P.F.; Nichols, D.E. [^{3}H]monoamine releasing and uptake inhibition properties of 3,4-methylenedioxymethamphetamine and p-chloroamphetamine analogues. *Eur. J. Pharmacol.*, **1991**, *200*, 9-16.

[2] Fitzgerald, J.L.; Reid, J.J. Effects of methylenedioxymethamphetamine on the release of monoamines from rat brain slices. *Eur. J. Pharmacol.*, **1990**, *191*, 217-220.

[3] Johnson, M.P.; Hoffman, A.J.; Nichols, D.E. Effects of the enantiomers of MDA, MDMA and related analogues on [^{3}H]serotonin and [^{3}H]dopamine release from superfused rat brain slices. *Eur. J. Pharmacol.*, **1986**, *132*, 269-276.

[4] Schmidt, C.J.; Levin, J.A.; Lovenberg, W. *In vitro* and *in vivo* neurochemical effects of methylenedioxymethamphetamine on striatal monoaminergic systems in the rat brain. *Biochem. Pharmacol.*, **1987**, *36*, 747-755.

[5] Rothman, R.B.; Baumann, M.H. Monoamine transporters and psychostimulant drugs. *Eur. J. Pharmacol.*, **2003**, *479*, 23-40.

[6] Han, D.D.; Gu, H.H. Comparison of the monoamine transporters from human and mouse in their sensitivities to psychostimulant drugs. *BMC Pharmacol.*, **2006**, *6*, 6.

[7] Gudelsky, G.A.; Yamamoto, B.K.; Nash, J.F. Potentiation of 3,4-methylenedioxymethamphetamine-induced dopamine release and serotonin neurotoxicity by 5-HT$_2$ receptor agonists. *Eur. J. Pharmacol.*, **1994**, *264*, 325-330.

[8] Yamamoto, B.K.; Nash, J.F.; Gudelsky, G.A. Modulation of methylenedioxymethamphetamine-induced striatal dopamine release by the interaction between serotonin and gamma-aminobutyric acid in the substantia nigra. *J. Pharmacol. Exp. Ther.*, **1995**, *273*, 1063-1070.

[9] Koch, S.; Galloway, M.P. MDMA induced dopamine release *in vivo*: role of endogenous serotonin. *J. Neural Transm.*, **1997**, *104*, 135-146.

[10] Baumann, M.H.; Clark, R.D.; Rothman, R.B. Locomotor stimulation produced by 3,4-methylenedioxymethamphetamine (MDMA) is correlated with dialysate levels of serotonin and dopamine in rat brain. *Pharmacol. Biochem. Behav.*, **2008**, *90*, 208-217.

[11] Gudelsky, G.A.; Nash, J.F. Carrier-mediated release of serotonin by 3,4-methylenedioxymethamphetamine: implications for serotonin-dopamine interactions. *J. Neurochem.*, **1996**, *66*, 243-249.

[12] Nair, S.G.; Gudelsky, G.A. Protein kinase C inhibition differentially affects 3,4-methylenedioxymethamphetamine-induced dopamine release in the striatum and prefrontal cortex of the rat. *Brain Res.*, **2004**, *1013*, 168-173.

[13] Trigo, J.M.; Renoir, T.; Lanfumey, L.; Hamon, M.; Lesch, K.P.; Robledo, P.; Maldonado, R. 3,4-methylenedioxymethamphetamine self-administration is abolished in serotonin transporter knockout mice. *Biol. Psychiatry*, **2007**, *62*, 669-679.

[14] Nash, J.F.; Brodkin, J. Microdialysis studies on 3,4-methylenedioxymethamphetamine-induced dopamine release: effect of dopamine uptake inhibitors. *J. Pharmacol. Exp. Ther.*, **1991**, *259*, 820-825.

[15] Shankaran, M.; Yamamoto, B.K.; Gudelsky, G.A. Mazindol attenuates the 3,4-methylenedioxymethamphetamine-induced formation of hydroxyl radicals and long-term depletion of serotonin in the striatum. *J. Neurochem.*, **1999**, *72*, 2516-2522.

[16] Nash, J.F. Ketanserin pretreatment attenuates MDMA-induced dopamine release in the striatum as measured by *in vivo* microdialysis. *Life Sci.*, **1990**, *47*, 2401-2408.

[17] Schmidt, C.J.; Sullivan, C.K.; Fadayel, G.M. Blockade of striatal 5-hydroxytryptamine2 receptors reduces the increase in extracellular concentrations of dopamine produced by the amphetamine analogue 3,4-methylenedioxymethamphetamine. *J. Neurochem.*, **1994**, *62*, 1382-1389.

[18] Bengel, D.; Murphy, D.L.; Andrews, A.M.; Wichems, C.H.; Feltner, D.; Heils, A.; Mossner, R.; Westphal, H.; Lesch, K.P. Altered brain serotonin homeostasis and locomotor insensitivity to 3, 4-methylenedioxymethamphetamine ("Ecstasy") in serotonin transporter-deficient mice. *Mol. Pharmacol.*, **1998**, *53*, 649-655.

[19] Peng, W.; Simantov, R. Altered gene expression in frontal cortex and midbrain of 3,4-methylenedioxymethamphetamine (MDMA) treated mice: differential regulation of GABA transporter subtypes. *J. Neurosci. Res.*, **2003**, *72*, 250-258.

[20] Giros, B.; Jaber, M.; Jones, S.R.; Wightman, R.M.; Caron, M.G. Hyperlocomotion and indifference to cocaine and amphetamine in mice lacking the dopamine transporter. *Nature*, **1996**, *379*, 606-612.

[21] Sora, I.; Wichems, C.; Takahashi, N.; Li, X.F.; Zeng, Z.; Revay, R.; Lesch, K.P.; Murphy, D.L.; Uhl, G.R. Cocaine reward models: conditioned place preference can be established in dopamine- and in serotonin-transporter knockout mice. *Proc. Natl. Acad. Sci. USA*, **1998**, *95*, 7699-7704.

[22] Ralph, R.J.; Paulus, M.P.; Fumagalli, F.; Caron, M.G.; Geyer, M.A. Prepulse inhibition deficits and perseverative motor patterns in dopamine transporter knock-out mice: differential effects of D1 and D2 receptor antagonists. *J. Neurosci.*, **2001**, *21*, 305-313.

[23] Powell, S.B.; Lehmann-Masten, V.D.; Paulus, M.P.; Gainetdinov, R.R.; Caron, M.G.; Geyer, M.A. MDMA "ecstasy" alters hyperactive and perseverative behaviors in dopamine transporter knockout mice. *Psychopharmacology (Berl)*, **2004**, *173*, 310-317.

[24] Franklin, K.B.J., Paxinos, G. *The mouse brain in stereotaxic coordinates.* Academic Press: San Diego, **1997**.

[25] Shen, H.W.; Hagino, Y.; Kobayashi, H.; Shinohara-Tanaka, K.; Ikeda, K.; Yamamoto, H.; Yamamoto, T.; Lesch, K.P.; Murphy, D.L.; Hall, F.S.; Uhl, G.R.; Sora, I. Regional differences in extracellular dopamine and serotonin assessed by *in vivo* microdialysis in mice lacking dopamine and/or serotonin transporters. *Neuropsychopharmacology*, **2004**, *29*, 1790-1799.

[26] Schmidt, C.J.; Lovenberg, W. *In vitro* demonstration of dopamine uptake by neostriatal serotonergic neurons of the rat. *Neurosci. Lett.*, **1985**, *59*, 9-14.

[27] Faraj, B.A.; Olkowski, Z.L.; Jackson, R.T. Active [^{3}H]-dopamine uptake by human lymphocytes: correlates with serotonin transporter activity. *Pharmacology*, **1994**, *48*, 320-327.

[28] Carboni, E.; Tanda, G.L.; Frau, R.; Di Chiara, G. Blockade of the noradrenaline carrier increases extracellular dopamine concentrations in the prefrontal cortex: evidence that dopamine is taken up *in vivo* by noradrenergic terminals. *J. Neurochem.*, **1990**, *55*, 1067-1070.

[29] Yamamoto, B.K.; Novotney, S. Regulation of extracellular dopamine by the norepinephrine transporter. *J. Neurochem.*, **1998**, *71*, 274-280.

[30] Moron, J.A.; Brockington, A.; Wise, R.A.; Rocha, B.A.; Hope, B.T. Dopamine uptake through the norepinephrine transporter in brain regions with low levels of the dopamine transporter: evidence from knock-out mouse lines. *J. Neurosci.*, **2002**, *22*, 389-395.

[31] Zhou, F.C.; Lesch, K.P.; Murphy, D.L. Serotonin uptake into dopamine neurons *via* dopamine transporters: a compensatory alternative. *Brain Res.*, **2002**, *942*, 109-119.

[32] Daws, L.C.; Montanez, S.; Owens, W.A.; Gould, G.G., Frazer, A.; Toney, G.M.; Gerhardt, G.A. Transport mechanisms governing serotonin clearance *in vivo* revealed by high-speed chronoamperometry. *J. Neurosci. Methods*, **2005**, *143*, 49-62.

[33] Liechti, M.E.; Baumann, C.; Gamma, A.; Vollenweider, F.X. Acute psychological effects of 3,4-methylenedioxymethamphetamine (MDMA, "Ecstasy") are attenuated by the serotonin uptake inhibitor citalopram. *Neuropsychopharmacology*, **2000**, *22*, 513-521.

[34] Liechti, M.E.; Saur, M.R.; Gamma, A.; Hell, D.; Vollenweider, F.X. Psychological and physiological effects of MDMA ("Ecstasy") after pretreatment with the 5-HT(2) antagonist ketanserin in healthy humans. *Neuropsychopharmacology*, **2000**, *23*, 396-404.

Received: October 01, 2009 Revised: April 17, 2010 Accepted: May 26, 2010

Enhanced Hyperthermia Induced by MDMA in Parkin Knockout Mice

Y. Takamatsu[1], H. Shiotsuki[1,2], S. Kasai[1], S. Sato[2], T. Iwamura[3], N. Hattori[2] and K. Ikeda[1,*]

[1]*Division of Psychobiology, Tokyo Institute of Psychiatry, 2-1-8 Kamikitazawa, Setagaya-ku, Tokyo 156-8585, Japan;*
[2]*Department of Neurology, Juntendo University School of Medicine, 2-1-1 Hongo, Bunkyou-ku, Tokyo 113-8421, Japan;*
[3]*Matsuyama University College of Pharmaceutical Sciences, 4-2 Bunkyo-cho, Matsuyama, Ehime 790-8578, Japan*

Abstract: MDMA (3,4-methylenedioxymethamphetamine) is reportedly severely toxic to both dopamine (DA) and serotonin neurons. MDMA significantly reduces the number of DA neurons in the substantia nigra, but not in the nucleus accumbens, indicating that MDMA causes selective destruction of DA neurons in the nigrostriatal pathway, sparing the mesolimbic pathway. Parkinson's disease (PD) is a neurodegenerative disorder of multifactorial origin. The pathological hallmark of PD is the degeneration of DA neurons in the nigrostriatal pathway. Mutations in the parkin gene are frequently observed in autosomal recessive parkinsonism in humans. Parkin is hypothesized to protect against neurotoxic insult, and we attempted to clarify the role of parkin in MDMA-induced hyperthermia, one of the causal factors of neuronal damage, using parkin knockout mice. Body temperature was measured rectally before and 15, 30, 45, and 60 min after intraperitoneal injection of MDMA (30 mg/kg) at an ambient temperature of 22 ± 2°C. Significantly enhanced hyperthermia after MDMA injection was observed in heterozygous and homozygous parkin knockout mice compared with wildtype mice, suggesting that parkin plays a protective role in MDMA neurotoxicity.

Keywords: Hyperthermia, knockout, mice, MDMA, parkin.

INTRODUCTION

The amphetamine derivative 3,4-methylenedioxymethamphetamine (MDMA) is abused by young adults despite its potentially neurotoxic effects and psychiatric complications. MDMA produces a rapid enhancement of serotonin and dopamine (DA) release in the brain [1, 2]. Administration of MDMA in mice is well known to produce acute hyperthermia and degeneration of striatal DA nerve terminals [3]. Recently, Granado and colleagues [4] reported that MDMA produces a significant decrease in the number of tyrosine hydroxylase (TH)-immunoreactive neurons in the substantia nigra. This decrease was accompanied by a dose-dependent decrease in TH- and DA transporter (DAT)-immunoreactivity in the striatum. MDMA significantly reduces TH- and DAT-immunoreactivity in the striatum, but not in the nucleus accumbens, indicating that MDMA causes selective destruction of DA neurons in the nigrostriatal pathway, sparing the mesolimbic pathway. The degree of long-term neurodegeneration produced by MDMA appears to be closely related to the magnitude of the hyperthermic response [5]. Attenuation of the hyperthermia alleviates MDMA-induced loss of striatal dopamine [3].

Parkinson's disease (PD) is the most common neurodegenerative movement disorder. The major pathological hallmark of PD is the degeneration of DAergic neurons in the substantia nigra that innervate the striatum. The major symptoms of PD include tremor, bradykinesia, cogwheel rigidity, and postural instability, which arise from the degeneration of DAergic neurons in the substantia nigra. PD is a neurodegenerative disorder of multifactorial origin, and mutations in the gene encoding parkin, an E3 ubiquitin-protein ligase [6], are frequently observed in autosomal recessive parkinsonism in humans. The loss of parkin function has been suggested to result in aberrant accumulation of parkin substrate proteins [6]. Accumulation of these proteins has been postulated to confer toxicity to DAergic neurons in the substantia nigra [7].

In the present study, we hypothesized that parkin protects against neurotoxic insult, and we attempted to clarify the role of parkin in MDMA-induced hyperthermia, one of the causal factors of neuronal damage, using parkin knockout mice.

MATERIALS AND METHODS

Mice

Wildtype, heterozygous, and homozygous parkin knockout mice were prepared from heterozygous/heterozygous parkin knockout mouse crosses (21-37 g, 12-29 weeks of age). Mice were housed in an animal facility maintained at 22 ± 2°C and 55 ± 5% relative humidity under a 12/12 h light/dark cycle with lights on at 8:00 a.m. Food and water were available *ad libitum*. All behavioral testing was conducted during the light cycle. The experimental procedures and housing conditions were approved by the Institutional Animal Care and Use Committee of the Tokyo Institute of Psychiatry, and all animals were treated humanely in accordance with our institutional animal experimentation guidelines.

Body Temperature Measurement

Rectal temperature measurement was performed using a digital thermometer (BAT-12; Physitemp Instruments Inc.,

*Address correspondence to this author at the Division of Psychobiology, Tokyo Institute of Psychiatry, 2-1-8 Kamikitazawa, Setagaya-ku, Tokyo 156-8585, Japan; Tel: +81-3-3304-5701, ext; 508; Fax: +81-3-3329-8035; E-mail: ikeda-kz@igakuken.or.jp

1570-159X/11 $58.00+.00

Clifton, NJ, USA) with 0.1°C accuracy and a rectal probe for mice (RET-3, Physitemp Instrument Inc.). Each mouse was lightly restrained by hand for approximately 20 s while the probe was inserted approximately 2 cm into the rectum and a steady reading was obtained. Body temperature was measured rectally before and 15, 30, 45, and 60 min after intraperitoneal (i.p.) injection of MDMA (30 mg/kg) at an ambient temperature of 22 ± 2°C.

Drugs

MDMA was synthesized at Matsuyama University College of Pharmaceutical Sciences and freshly dissolved in saline. MDMA and vehicle were administered in a volume of 0.1 ml/10 g body weight.

Statistical Analysis

Mean and standard error were calculated from the values of 12-17 subjects. Changes in body temperature were analyzed by repeated-measures analysis of variance (ANOVA) followed by Scheffe's *post hoc* test. Baseline temperature and changes in body temperature areas-under-the-curve (AUC) were analyzed by one-way ANOVA and Scheffe's *post hoc* test.

RESULTS

Baseline Body Temperature in Parkin Knockout Mice

Baseline body temperature was measured before MDMA injection at room temperature (22 ± 2°C). No significant difference in baseline body temperature was observed among wildtype, heterozygous, and homozygous parkin knockout mice (Fig. **1**).

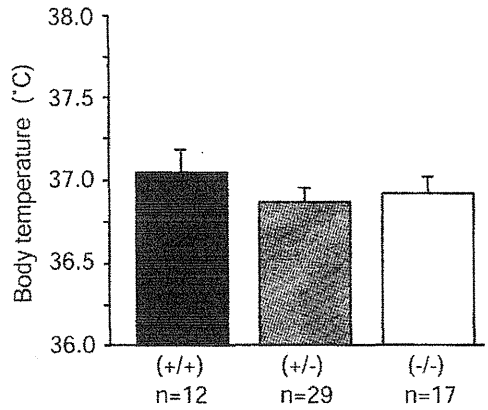

Fig. (1). No significant differences in baseline body temperature were observed among wildtype, heterozygous, and homozygous parkin knockout mice. Body temperature prior to MDMA injection did not significantly differ among genotypes. Baseline body temperature was analyzed by one-way ANOVA ($F_{2,55}$ = 0.629, p = 0.5369) at an ambient temperature of 22 ± 2°C.

No Sex Differences in MDMA-Induced Hyperthermia

Body temperature was measured 15, 30, 45, and 60 min after i.p. injection of MDMA (30 mg/kg) at an ambient temperature of 22 ± 2°C. No significant differences in MDMA-induced hyperthermia were observed between males and females within each genotype (Fig. **2**).

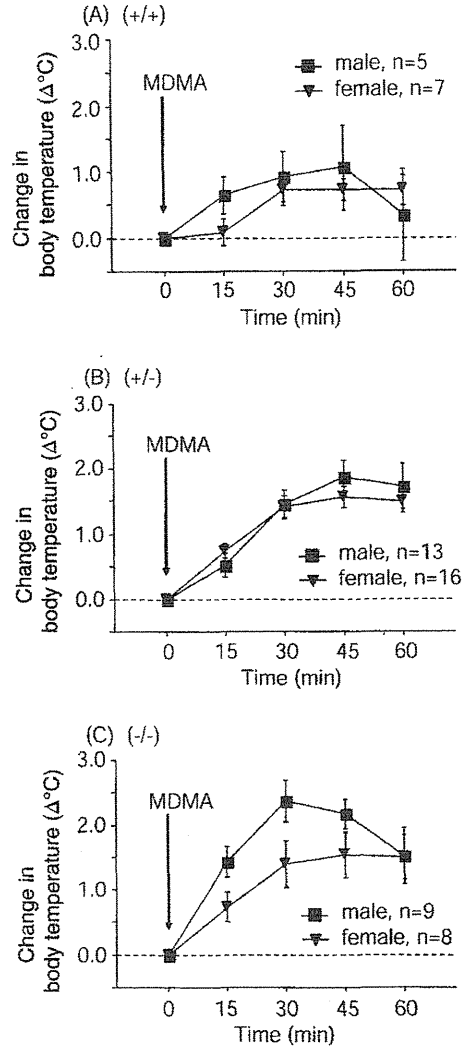

Fig. (2). Similar MDMA-induced (30 mg/kg, i.p.) hyperthermia was observed in male and female mice within each genotype. Body temperature areas-under-the-curve were analyzed by repeated-measures ANOVA. (**A**) Sex, $F_{1,10}$ = 0.181, p = 0.6796; Time, $F_{4,40}$ = 4.741, p = 0.0032; Sex × Time interaction, $F_{4,40}$ = 1.124, p = 0.3587. (**B**) Sex, $F_{1,27}$ = 0.134, p = 0.7170; Time, $F_{4,108}$ = 62.705, p < 0.0001; Sex × Time interaction, $F_{4,108}$ = 1.231, p = 0.3021. (**C**) Sex, $F_{1,15}$ = 2.350, p = 0.1461; Time, $F_{4,60}$ = 26.22, p < 0.0001; Sex × Time interaction, $F_{4,60}$ = 2.059, p = 0.0974.

Enhancement of MDMA-Induced Hyperthermia in Parkin Knockout and Heterozygous Mice

Body temperature gradually increased from baseline after MDMA injection in all genotype groups. MDMA significantly enhanced hyperthermia from 15 to 45 min after injection in parkin knockout mice and from 45 to 60 min after injection in heterozygous mice compared with wildtype mice (Fig. **3A**). MDMA produced hyperthermia, with a maximum increase of 0.9°C (37.9°C) 45 min after injection in wildtype mice, 1.7°C (38.6°C) 45 min after injection in heterozygous mice, and 1.9°C (38.8°C) 30 min after injection in parkin knockout mice. Body temperature AUC values reflected significantly enhanced hyperthermia in parkin knockout and heterozygous mice compared with wildtype mice (Fig. **3B**).

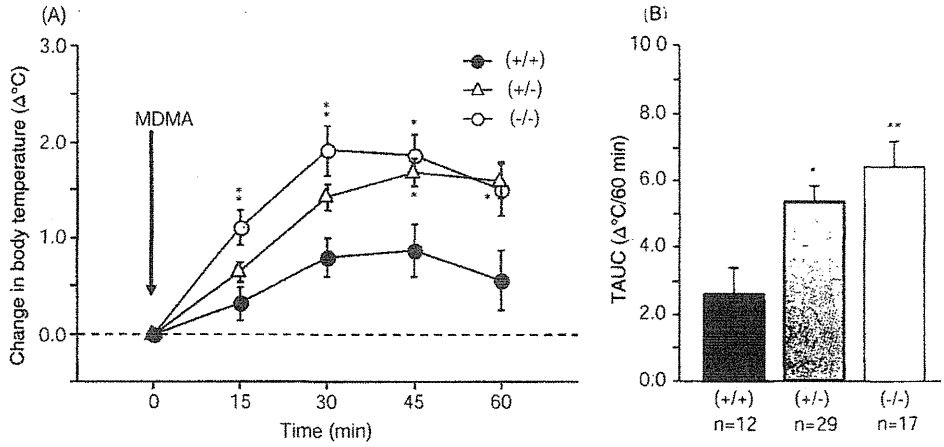

Fig. (3). Enhanced MDMA-induced hyperthermia in heterozygous and homozygous parkin knockout mice compared with wildtype mice. (**A**) Change in body temperature in mice injected with MDMA (30 mg/kg, i.p.). Body temperature areas-under-the-curve were analyzed by repeated-measures ANOVA (Genotype, $F_{2,55} = 6.746$, $p = 0.0024$; Time, $F_{4,220} = 61.267$, $p < 0.0001$; Genotype × Time interaction, $F_{8,220} = 3.664$, $p = 0.0005$) followed by Scheffe's *post hoc* test (*$p < 0.05$, **$p < 0.01$). (**B**) Change in body temperature areas-under-the-curve (TAUC) shown as an integration of the temperature *vs.* time curve shown in panel A. TAUC values were analyzed by one-way ANOVA ($F_{2,55} = 6.746$, $p = 0.0024$) followed by Scheffe's *post hoc* test (*$p < 0.05$, **$p < 0.01$).

DISCUSSION

In the present study, significantly enhanced MDMA-induced hyperthermia was observed in parkin knockout and heterozygous mice compared with wildtype mice (Fig. **3B**). The enhanced MDMA-induced hyperthermia in parkin knockout mice supports the hypothesis that parkin protects against MDMA-induced neurotoxic insult.

Hyperthermia is one of the major symptoms of acute MDMA-induced toxicity, which has been shown to be affected by body temperature [3]. MDMA produces a rapid enhancement of DA release in the striatum [1] and preoptic anterior hypothalamus [8]. MDMA-induced hyperthermia was blocked by a DA D_1 receptor antagonist [9]. Moreover, both the hyperthermia and augmented DA levels in the preoptic anterior hypothalamus after i.p. MDMA injection were significantly reduced by pretreatment with a D_1 antagonist [8]. Interestingly, Sato *et al.* (2006) [10] reported that D_1 receptor levels in the striatum in parkin knockout mice was higher than in wildtype mice, although no change in TH-positive substantia nigra neurons was found in parkin knockout mice, and no significant decrease in DAT levels was observed in the striatum. Therefore, the enhanced MDMA-induced hyperthermia observed in the present study may be attributable to increased levels of D_1 receptors in parkin knockout mice.

Sato *et al.* (2006) [10] also suggested that presynaptic neurons (i.e., DAergic neurons) are functionally impaired in parkin knockout mice. DA synthesis is significantly decreased and methamphetamine-induced DA release is reduced in parkin knockout mice. Considering that DAergic neurons in the substantia nigra are severely damaged in PD patients, the enhanced MDMA-induced hyperthermia in parkin knockout mice may be attributable to functional impairment of DAergic neurons, although the relationship between hyperthermia and DAergic neuron dysfunction remains to be elucidated.

Additionally, we found no significant difference in baseline body temperature among wildtype, heterozygous, and homozygous parkin knockout mice (Fig. **1**). These data suggest that parkin does not play a crucial role in the system that maintains basal body temperature.

In conclusion, MDMA-induced hyperthermia was enhanced in parkin knockout and heterozygous mice compared with wildtype mice. Parkin is hypothesized to be critical for protecting DAergic neurons from toxic insult, and the present results suggest that parkin plays a protective role against MDMA-induced DAergic neuron neurotoxicity.

ACKNOWLEDGEMENTS

We acknowledge Mr. Michael Arends for his assistance with editing the manuscript and Ms. Junko Hasegawa for her assistance with genotyping mice. This work was supported by a research grant (17025054) from the MEXT of Japan, by grants from the MHLW of Japan (H17-pharmaco-001, H19-iyaku-023, and 18A-3 and 19A-8 for Nervous and Mental Disorders), by a grant from the Smoking Research Foundation, and by a grant from the Mitsubishi Foundation for Social Welfare Activities.

ABBREVIATIONS

ANOVA	=	Analysis of variance
DA	=	Dopamine
DAT	=	Dopamine transporter
MDMA	=	3,4-methylenedioxymethamphetamine
PD	=	Parkinson's disease
TH	=	Tyrosine hydroxylase

REFERENCES

[1] Camarero, J.; Sanchez, V.; O'Shea, E.; Green, A.R.; Colado, M.I. Studies, using *in vivo* microdialysis, on the effect of the dopamine uptake inhibitor GBR 12909 on 3,4-methylenedioxymethamphetamine ("ecstasy")-induced dopamine release and free radical formation in the mouse striatum. *J. Neurochem.*, **2002**, *81*, 961-972.

[2] Doly, S.; Valjent, E.; Setola, V.; Callebert, J.; Hervé, D.; Launay, J.M.; Maroteaux, L. Serotonin 5-HT_{2B} receptors are required for

3,4-methylenedioxymethamphetamine-induced hyperlocomotion and 5-HT release *in vivo* and *in vitro*. *J. Neurosci.*, **2008**, *28*, 2933-2940.

[3] Colado, M.I.; Camarero, J.; Mechan, A.O.; Sanchez, V.; Esteban, B.; Elliott, J.M.; Green, A.R. A study of the mechanisms involved in the neurotoxic action of 3,4-methylenedioxymethamphetamine (MDMA, "ecstasy") on dopamine neurones in mouse brain. *Br. J. Pharmacol.*, **2001**, *134*, 1711-1723.

[4] Granado, N.; O'Shea, E.; Bove, J.; Vila, M.; Colado, M.I.; Moratalla, R. Persistent MDMA-induced dopaminergic neurotoxicity in the striatum and substantia nigra of mice. *J. Neurochem.*, **2008**, *107*, 1102-1112.

[5] Malberg, J.E.; Seiden, L.S. Small changes in ambient temperature cause large changes in 3,4-methylenedioxymethamphetamine (MDMA)-induced serotonin neurotoxicity and core body temperature in the rat. *J. Neurosci.*, **1998**, *18*, 5086-5094.

[6] Shimura, H.; Hattori, N.; Kubo, S.; Mizuno, Y.; Asakawa, S.; Minoshima, S.; Shimizu, N.; Iwai, K.; Chiba, T.; Tanaka, K.; Suzuki, T. Familial Parkinson disease gene product, parkin, is a ubiquitin-protein ligase. *Nat. Genet.*, **2000**, *25*, 302-305.

[7] Xu, J.; Kao, S.Y.; Lee, F.J.; Song, W.; Jin, L.W.; Yankner, B.A. Dopamine-dependent neurotoxicity of α-synuclein: a mechanism for selective neurodegeneration in Parkinson disease. *Nat. Med.*, **2002**, *8*, 600-606.

[8] Benamar, K.; Geller, E.B.; Adler, M.W. A new brain area affected by 3,4-methylenedioxymethamphetamine: a microdialysis-biotelemetry study. *Eur. J. Pharmacol.*, **2008**, *596*, 84-88.

[9] Mechan, A.O.; Esteban, B.; O'Shea, E.; Elliott, J.M.; Colado, M.I.; Green, A.R. The pharmacology of the acute hyperthermic response that follows administration of 3,4-methylenedioxymethamphetamine (MDMA, "ecstasy") to rats. *Br. J. Pharmacol.*, **2002**, *135*, 170-180.

[10] Sato, S.; Chiba, T.; Nishiyama, S.; Kakiuchi, T.; Tsukada, H.; Hatano, T.; Fukuda, T.; Yasoshima, Y.; Kai, N.; Kobayashi, K.; Mizuno, Y.; Tanaka, K.; Hattori, N. Decline of striatal dopamine release in parkin-deficient mice shown by *ex vivo* autoradiography. *J. Neurosci. Res.*, **2006**, *84*, 1350-1357.

Received: October 01, 2009 Revised: April 17, 2010 Accepted: May 26, 2010

Identification of Selective Agonists and Antagonists to G Protein-Activated Inwardly Rectifying Potassium Channels: Candidate Medicines for Drug Dependence and Pain

D. Nishizawa[1], N. Gajya[2] and K. Ikeda[1,*]

[1]*Division of Psychobiology, Tokyo Institute of Psychiatry, Tokyo;* [2]*Discovery Biology-1, Discovery Biology Research, Global Research & Development, Nagoya Laboratories, Pfizer Japan Inc, Nagoya, Japan*

Abstract: G protein-activated inwardly rectifying K^+ (GIRK) channels have been known to play a key role in the rewarding and analgesic effects of opioids. To identify potent agonists and antagonists to GIRK channels, we examined various compounds for their ability to activate or inhibit GIRK channels. A total of 503 possible compounds with low molecular weight were selected from a list of fluoxetine derivatives at Pfizer Japan Inc. We screened these compounds by a *Xenopus* oocyte expression system. GIRK1/2 and GIRK1/4 heteromeric channels were expressed on *Xenopus laevis* oocytes at Stage V or VI. A mouse IRK2 channel, which is another member of inwardly rectifying potassium channels with similarity to GIRK channels, was expressed on the oocytes to examine the selectivity of the identified compounds to GIRK channels. For electrophysiological analyses, a two-electrode voltage clamp method was used. Among the 503 compounds tested, one compound and three compounds were identified as the most effective agonist and antagonists, respectively. All of these compounds induced only negligible current responses in the oocytes expressing the IRK2 channel, suggesting that these compounds were selective to GIRK channels. These effective and GIRK-selective compounds may be useful possible therapeutics for drug dependence and pain.

Keywords: G protein-activated inwardly rectifying K^+ (GIRK, Kir3) channels, Kir channel, agonist, antagonist, Pfizer compounds, *Xenopus* oocyte.

INTRODUCTION

G protein-activated inwardly rectifying K^+ (GIRK) channels, also named as Kir3 channels, are members of the inwardly rectifying potassium channel family. GIRK channels are activated by several $G_{i/o}$ protein-coupled receptors, such as opioid receptors, which causes hyperpolarization of the neurons involved and thus leads to inhibitory regulation. GIRK channels are expressed in many tissues with different subunit compositions [1-3]. In the heart, the GIRK4 subunit is abundantly expressed as a homomultimer or heteromultimer with GIRK1 and is involved in heart rate regulation [4, 5]. In the central nervous system, GIRK channels are mainly expressed as a GIRK1/2 heteromultimer in most regions and as a GIRK2 homomultimer in the substantia nigra and ventral tegmental area. GIRK channels play a key role in analgesia [6], as demonstrated in studies using GIRK channel subunit knockout mice [7-11]. Further, mice lacking the GIRK2 or GIRK3 subunit show decreased cocaine self-administration, suggesting decreased reinforcing effects of cocaine in these mice [12] and hence the involvement of GIRK channels in its rewarding effects.

Therefore, GIRK channel inhibitors may be possible candidates as therapeutic drugs to treat substance dependence. Drugs that selectively open GIRK channels may be expected to exhibit analgesic effects without impacting opioidergic intracellular signaling pathways and $G_{i/o}$ proteins and thus have fewer side effects. It has been known that various compounds inhibit GIRK channels [13-17], but only a few have thus far been shown to activate the GIRK channel [18-20]. To identify more potent GIRK channel agonists and antagonists, we examined the ability of various compounds to activate or inhibit GIRK channels.

*Address correspondence to this author at the Director, Molecular Psychiatry Research Tokyo Institute of Psychiatry 2-1-8 Kamikitazawa, Setagaya-ku, Tokyo 156-8585, Japan; Tel: +81-3-3304-5701; Fax: +81-3-3329-8035; E-mail: ikeda-kz@igakuken.or.jp

METHODS

Compounds

To search for selective GIRK channel agonists and antagonists, a total of 503 possible compounds with low molecular weight were selected from a list of fluoxetine derivatives at Pfizer Japan Inc. The specific names and detailed properties of each compound are not available to the public. For convenience, the compounds were numbered from PF 1 to PF 503. All drugs were dissolved in dimethyl sulfoxide (DMSO).

Electrophysiological Analysis

To screen the PF compounds, a *Xenopus* oocyte expression system was utilized based on a previous report [21]. In this system, murine GIRK1 (Kir3.1), GIRK2 (Kir3.2), and GIRK4 (Kir3.4) subunits were expressed as heteromeric channels of GIRK1/2 and GIRK1/4 in *Xenopus laevis* oocytes at Stage V or VI by coinjection of the cRNAs of mouse GIRK1 and GIRK2 subunits, and GIRK1 and GIRK4 subunits, respectively. The murine IRK2 (Kir2.1) channel,

1570-159X/11 $58.00+.00

which is a member of another inwardly rectifying potassium channel family with similarity to the GIRK channel family, was expressed in the oocytes to examine the selectivity of the identified compounds to GIRK channels. For electrophysiological analyses, a two-electrode voltage clamp (GeneClamp500, Axon Instruments) method was used with the membrane potential kept at -70 mV. A high potassium solution (96 mM KCl, 2 mM NaCl, 1 mM $MgCl_2$, 1.5mM $CaCl_2$, 5 mM HEPES) served as perfusion solution. Ethanol (100 mM) and $BaCl_2$ (2 mM) were used as positive controls for agonist and antagonist, respectively, and DMSO was used as a negative control. Oocytes without cRNA injection served as controls.

Assay Procedure

The procedure of the assay consisted of three steps. In the first step, among the total of 503 PF compounds, every four compounds were mixed together and dissolved in the high potassium solution to yield a solution containing each compound at 10 μM. Then the total of 126 solutions of pooled PF compounds were applied to the oocytes expressing the GIRK1/2 channel (n = 2), GIRK1/4 channel (n = 2), and oocyte controls (n = 2) without GIRK channel expression. After the first screening step, several pools of compounds were selected based on the following criteria: (i) stronger agonistic or antagonistic effect on GIRK channels, (ii) similar responses between the two oocytes tested, and (iii) substantial difference in the effect of activation or inhibition between GIRK1/2 and GIRK1/4 channels.

In the second step, PF compounds in the selected pools (10 μM) were separately applied to the oocytes expressing the GIRK1/2 channel (n = 2), GIRK1/4 channel (n = 2), and oocyte controls (n = 2) without GIRK channel expression. Several compounds were selected based on the same criteria as those in the first step, in which their magnitude of inhibition/activation and the selectivity for the GIRK1/2 or GIRK1/4 channel were considered.

In the third step, each selected PF compound was applied to the oocytes expressing the GIRK1/2 channel (n = 5) and GIRK1/4 channel (n = 5) at various concentrations to examine concentration-response relationships. Selectivity of the compounds for GIRK channels was tested by applying the compounds to the oocytes expressing IRK2 (n = 2) and oocyte controls (n = 2) without GIRK channel expression. Data were fitted to a standard regression equation by using KaleidaGraph 3.5J (HULINKS, Inc.) for analysis of concentration-response relationships.

Statistical Analyses

The current responses to PF compounds were normalized by those to ethanol or $BaCl_2$, which was applied to each oocyte like PF compounds. For statistical analyses, two-way analysis of variance (ANOVA) or Student's t-test was performed with the significance level set at $P < 0.05$. SPSS v.12.0J for Windows (LEAD Technologies, Inc.) was used for analyses.

RESULTS

In the first screening step, some pools of PF compounds showed agonistic effects on GIRK channels while most others showed antagonistic effects on GIRK1/2 and GIRK1/4 channels with various efficacies. All of the pools of PF compounds induced negligible responses in the oocytes without cRNA injection (data not shown), suggesting the current responses by PF compounds were caused by exogenously expressed GIRK channels. Based on the criteria described above, PF 9 – PF 12, PF 401 – PF 404, and PF 409 – PF 412 pools were selected as candidate agonists with relatively low percentage inhibition of GIRK currents compared to $BaCl_2$ responses, while PF 37 – PF 40, PF 157 – PF 160, PF 185 – PF 188, PF 233 – PF 236, and PF 245 – PF 248 pools were selected as candidate antagonists with relatively high percentage inhibition of GIRK currents (Fig. 1). In addition, the PF 417 – PF 420 pool was selected as candidate agonist or antagonist because it induced moderate inhibition of GIRK1/2 channels and almost no effect on GIRK1/4 channels (Fig. 1).

In the second screening step, the PF compounds in the nine pools selected above were separately applied to the oo-

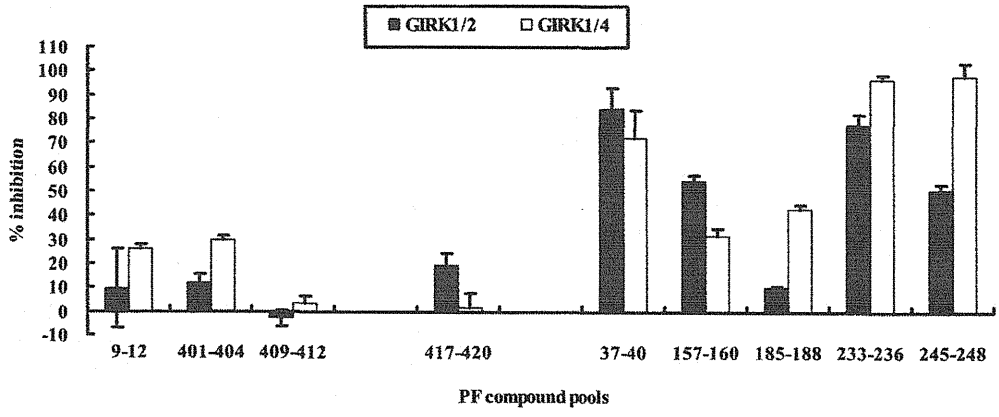

Fig. (1). Current Responses Induced by the Selected PF Compound Pools in the First Screening Step. Normalized current responses to the pools of PF compounds by the response to $BaCl_2$. PF 9 – PF 12, PF 401 – PF 404, and PF 409 – PF 412 pools were selected as candidate agonists, and PF 37 – PF 40, PF 157 – PF 160, PF 185 – PF 188, PF 233 – PF 236, and PF 245 – PF 248 pools were selected as candidate antagonists. The PF 417 – PF 420 pool was selected as a candidate agonist or antagonist in the first screening step.

cytes. While most of these individual PF compounds showed antagonistic effects or almost no effect on GIRK channels, only PF 419 showed an apparent agonistic effect on both GIRK1/2 and GIRK1/4 cannels (Fig. **2a**, **b**). Therefore, PF 419 was selected as a candidate agonist. In addition, PF 40, PF 236, and PF 246, which induced comparatively higher percentage inhibition of GIRK currents, were selected as candidate antagonists (Fig. **2b**).

In the third screening step, the four PF compounds selected above (PF 419, PF 40, PF 236, PF 246) were applied to the oocytes expressing the GIRK1/2 channel (n = 5) and GIRK1/4 channel (n = 5) at various concentrations. Considering the results in our preliminary experiments testing the effect of each compound at 0.1, 1, and 10 μM (data not shown), the concentrations of each compound to examine the concentration-response relationships were set at 1, 3, 10, 30, and 100 μM. Fig. (**3**) represents the concentration-response relationships for each PF compound. PF 419 activated GIRK currents dose-dependently, whereas PF 40, PF 236, and PF 246 inhibited them dose-dependently. Two-way ANOVA revealed that there were significant main effects of the concentrations of PF compounds on the current responses to PF 419 ($F_{4,40}$ = 8.606, P < 0.001), PF 40 ($F_{4,40}$ = 75.475, P < 0.001), PF 236 ($F_{4,40}$ = 80.160, P < 0.001), and PF 246 ($F_{4,40}$ = 227.702, P < 0.001). There were significant main effects of the GIRK subunit compositions on the current responses in PF 419 ($F_{1,40}$ = 6.078, P = 0.018), PF 40 ($F_{1,40}$ = 19.865, P < 0.001), and PF 236 ($F_{1,40}$ = 50.590, P < 0.001). Significant interactions were observed between the concentrations and GIRK subunit compositions in PF 40 ($F_{4,40}$ = 3.252, P = 0.021) and PF 236 ($F_{4,40}$ = 4.371, P = 0.005). *Post hoc* analysis revealed a significant difference between the GIRK1/2 and GIRK1/4 channels at 100 μM (P = 0.004) in PF 419, at 30 μM (P = 0.004) and 100 μM (P < 0.001) in PF 40, and at 10 μM (P = 0.001), 30 μM (P < 0.001), and 100 μM (P < 0.001) in PF 236 (Fig. **3**). Inhibition concentration (IC_{50}) values were calculated for PF 40, PF 236, and PF 246 (Table **1**). In addition, we examined the selectivity of these compounds for GIRK channels by applying them to oocytes expressing the IRK2 channel (n = 2). All four compounds showed almost no or negligible effects on IRK2 channels (data not shown), suggesting that these compounds were selective for GIRK channels.

DISCUSSION

In the first step of the screening process, most pools of PF compounds showed apparent antagonistic effects and a few showed agonistic effects on GIRK channels, possibly because the PF compounds used in the present assay were selected from the fluoxetine derivatives that are known to inhibit GIRK channels [22]. However, several pools of PF compounds exhibited almost no effects on GIRK channels. It

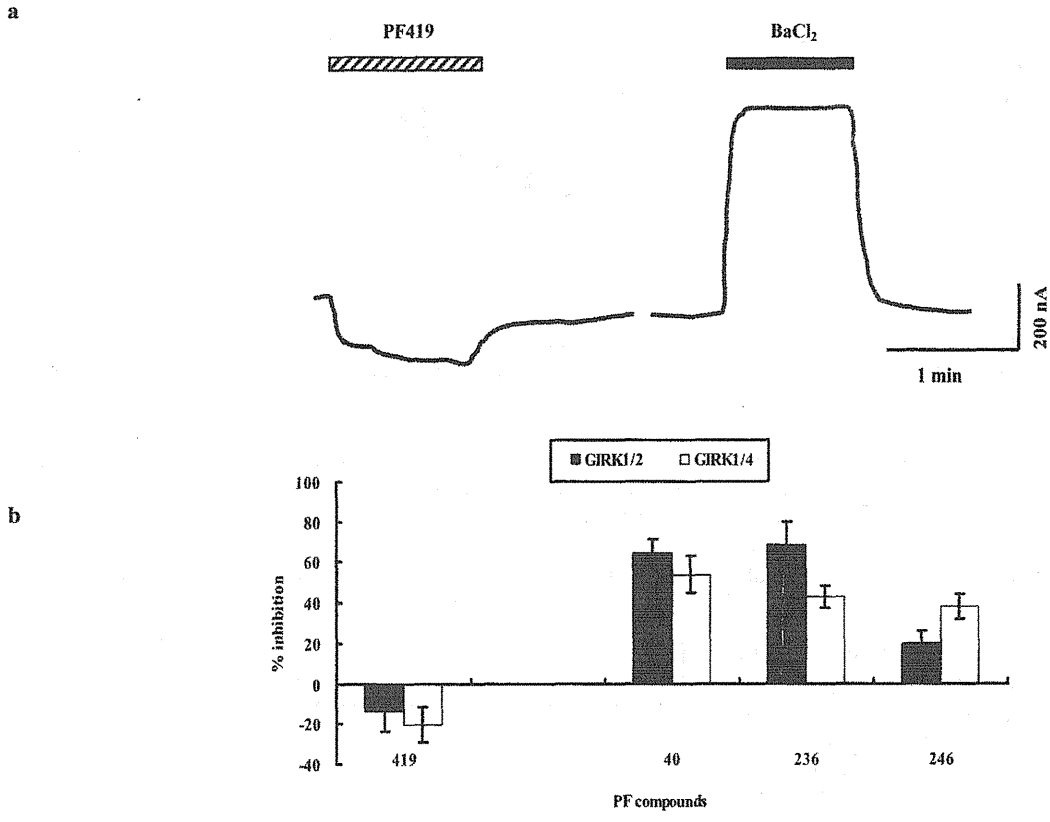

Fig. (2). Candidate Agonist and Antagonists Identified in the Second Screening Step. PF 419 was selected as a candidate agonist, and PF 40, PF 236, and PF 246 were selected as candidate antagonists in the second screening step. **a**. Traces of typical current responses to PF 419 (30 μM) and $BaCl_2$ (2 mM) in the oocyte expressing the GIRK1/4 channel. The striped and filled bars represent the duration of the application of PF 419 and $BaCl_2$, respectively. **b**. The normalized current responses to the selected PF compounds by the response to $BaCl_2$.

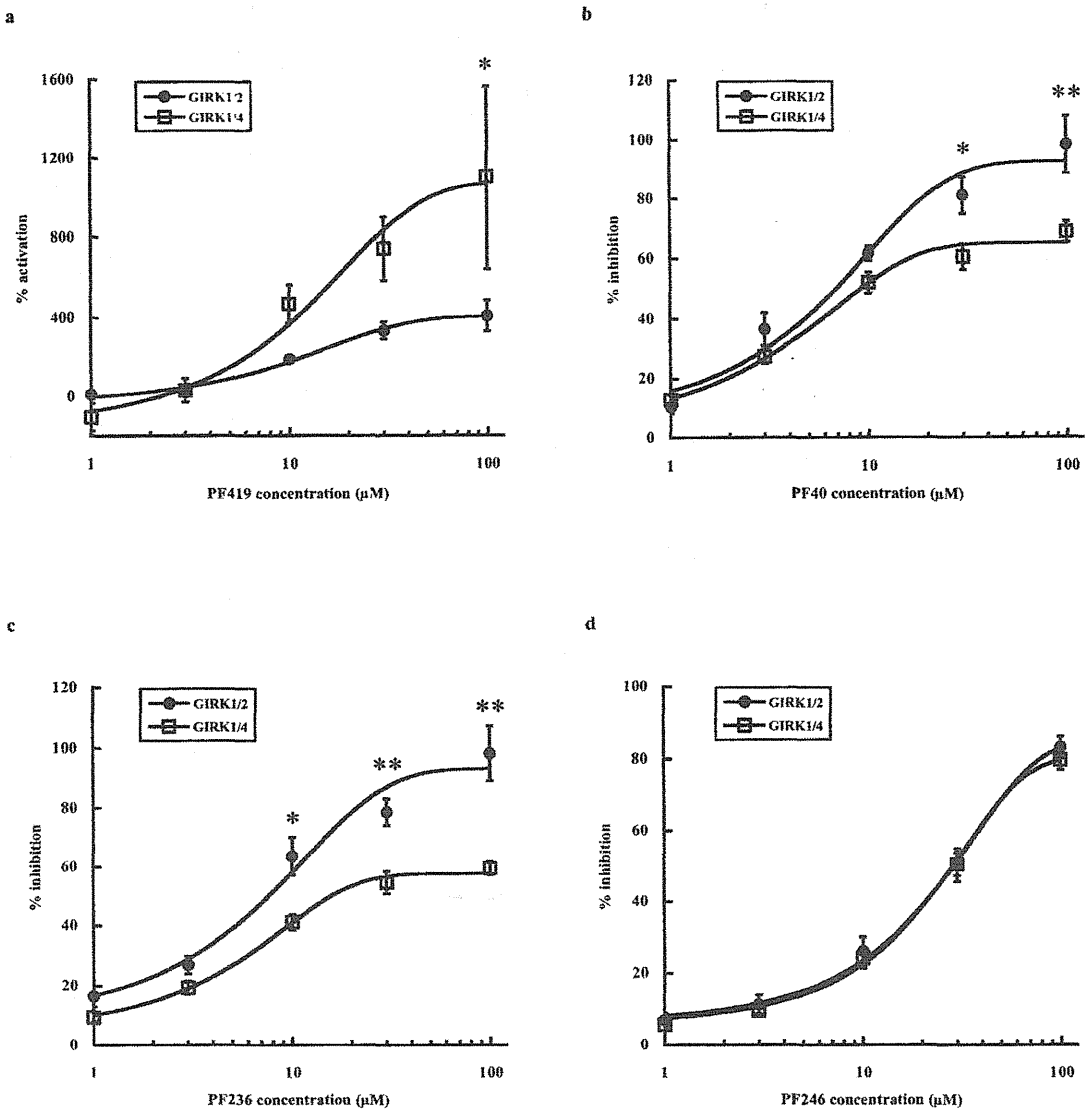

Fig. (3). Concentration-Response Relationships of the Identified Agonist and Antagonists to GIRK Channels. a. Current response was normalized by the response to ethanol (100 mM). **b-d.** Current responses were normalized by the response to $BaCl_2$ (2 mM). *$P < 0.005$ between GIRK1/2 and GIRK1/4. **$P < 0.001$ between GIRK1/2 and GIRK1/4.

might be possible that agonists and antagonists were combined in a pool which effectively negated their possible actions on GIRK channels. Therefore, if different combinations of PF compounds had been pooled, different agonists and antagonists might have been identified after the overall screening procedure.

As shown in Table 1, the IC_{50} values for PF 40, PF 236, and PF 246 calculated in the third screening step ranged from 5.98 to 31.2. These were comparable to, or lower than, those of various antipsychotic drugs [14-16], indicating they could be more potent antagonists than therapeutic drugs currently available. In addition, the agonistic effect of PF 419 at 10 μM or higher was several times that of ethanol (100 mM), a well-known GIRK agonist [18, 19], indicating that PF 419 is a very potent GIRK agonist. In a comparison between GIRK1/2 and GIRK1/4, significant differences were observed in PF 419, PF 40, and PF 236 (Fig. 3), suggesting that PF 40 and PF 236 are antagonists relatively selective to GIRK1/2 and PF 419 is an agonist relatively selective to GIRK1/4.

Table 1. IC_{50} Values of the Antagonists Selected in the Overall Screening

	PF40	PF236	PF246
GIRK1/2	6.06	5.98	24
(95%CI)	(4.03-8.68)	(3.09-10.3)	(13.4-55.6)
GIRK1/4	16.6	31.2	27.5
(95%CI)	(8.03-44.7)	(15.2-107)	(16.7-54.8)

CI: confidence intervals.

In conclusion, by screening a total of 503 PF compounds, one compound and three compounds were identified as the most effective agonist and antagonists, respectively. These compounds were all selective for GIRK channels. These effective and GIRK-selective compounds may be useful, therefore, as possible therapeutics for drug dependence and pain.

ACKNOWLEDGEMENTS

We are grateful to Dr. Toru Kobayashi for his instruction on the experimental techniques and methods of data analyses used in this study. This work was supported by a joint research fund from Pfizer Japan Inc.

REFERENCES

[1] Jelacic, T.M.; Kennedy, M.E.; Wickman, K.; Clapham, D.E. Functional and biochemical evidence for G-protein-gated inwardly rectifying K^+ (GIRK) channels composed of GIRK2 and GIRK3. *J. Biol. Chem.*, **2000**, *275*, 36211-36216.

[2] Kobayashi, T.; Ikeda, K.; Ichikawa, T.; Abe, S.; Togashi, S.; Kumanishi, T. Molecular cloning of a mouse G-protein-activated K^+ channel (mGIRK1) and distinct distributions of three GIRK (GIRK1, 2 and 3) mRNAs in mouse brain. *Biochem. Biophys. Res. Commun.*, **1995**, *208*, 1166-1173.

[3] Wickman, K.; Karschin, C.; Karschin, A.; Picciotto, M.R.; Clapham, D.E. Brain localization and behavioral impact of the G-protein-gated K^+ channel subunit GIRK4. *J. Neurosci.*, **2000**, *20*, 5608-5615.

[4] Corey, S.; Clapham., D.E. Identification of native atrial G-protein-regulated inwardly rectifying K^+ (GIRK4) channel homomultimers. *J. Biol. Chem.*, **1998**, *273*, 27499-27504.

[5] Wickman, K.; Nemec, J.; Gendler, S.J.; Clapham, D.E. Abnormal heart rate regulation in GIRK4 knockout mice. *Neuron*, **1998**, *20*, 103-114.

[6] Ikeda, K.; Kobayashi, T.; Kumanishi, T.; Yano, R.; Sora, I.; Niki, H. Molecular mechanisms of analgesia induced by opioids and ethanol: is the GIRK channel one of the keys? *Neurosci. Res.*, **2002**, *44*, 121-131.

[7] Blednov, Y.A.; Stoffel, M.; Alva, H.; Harris, R.A. A pervasive mechanism for analgesia: activation of GIRK2 channels. *Proc. Natl. Acad. Sci. USA*, **2003**, *100*, 277-282.

[8] Marker, C.L.; Cintora, S.C.; Roman, M.I.; Stoffel, M.; Wickman, K. Hyperalgesia and blunted morphine analgesia in G protein-gated potassium channel subunit knockout mice. *Neuroreport*, **2002**, *13*, 2509-2513.

[9] Marker, C.L.; Lujan, R.; Loh, H.H.; Wickman, K. Spinal G-protein-gated potassium channels contribute in a dose-dependent manner to the analgesic effect of μ- and δ- but not κ-opioids. *J. Neurosci.*, **2005**, *25*, 3551-3559.

[10] Marker, C.L.; Stoffel, M.; Wickman, K. Spinal G-protein-gated K^+ channels formed by GIRK1 and GIRK2 subunits modulate thermal nociception and contribute to morphine analgesia. *J. Neurosci.*, **2004**, *24*, 2806-2812.

[11] Mitrovic, I.; Margeta-Mitrovic, M.; Bader, S.; Stoffel, M.; Jan, L.Y.; Basbaum, A.I. Contribution of GIRK2-mediated postsynaptic signaling to opiate and α_2-adrenergic analgesia and analgesic sex differences. *Proc. Natl. Acad. Sci. USA*, **2003**, *100*, 271-276.

[12] Morgan, A.D.; Carroll, M.E.; Loth, A.K.; Stoffel, M.; Wickman, K. Decreased cocaine self-administration in Kir3 potassium channel subunit knockout mice. *Neuropsychopharmacology*, **2003**, *28*, 932-938.

[13] Kobayashi, T.; Ikeda, K.; Kumanishi., T. Effects of clozapine on the δ- and κ-opioid receptors and the G-protein-activated K^+ (GIRK) channel expressed in *Xenopus* oocytes. *Br. J. Pharmacol.*, **1998**, *123*, 421-426.

[14] Kobayashi, T.; Ikeda, K.; Kumanishi, T. Inhibition by various antipsychotic drugs of the G-protein-activated inwardly rectifying K^+ (GIRK) channels expressed in *Xenopus* oocytes. *Br. J. Pharmacol.*, **2000**, *129*, 1716-1722.

[15] Kobayashi, T.; Washiyama, K.; Ikeda, K. Inhibition of G protein-activated inwardly rectifying K^+ channels by various antidepressant drugs. *Neuropsychopharmacology*, **2004**, *29*, 1841-1851.

[16] Kobayashi, T.; Washiyama, K.; Ikeda, K. Modulators of G protein-activated inwardly rectifying K^+ channels: potentially therapeutic agents for addictive drug users. *Ann. NY Acad. Sci.*, **2004**, *1025*, 590-594.

[17] Kobayashi, T.; Washiyama, K.; Ikeda, K. Inhibition of G protein-activated inwardly rectifying K^+ channels by the antidepressant paroxetine. *J. Pharmacol. Sci.*, **2006**, *102*, 278-287.

[18] Kobayashi, T.; Ikeda, K.; Kojima, H.; Niki, H.; Yano, R.; Yoshioka, T.; Kumanishi, T. Ethanol opens G-protein-activated inwardly rectifying K^+ channels. *Nat. Neurosci.*, **1999**, *2*, 1091-1097.

[19] Lewohl, J.M.; Wilson, W.R.; Mayfield, R.D.; Brozowski, S.J.; Morrisett, R.A.; Harris, R.A. G-protein-coupled inwardly rectifying potassium channels are targets of alcohol action. *Nat. Neurosci.*, **1999**, *2*, 1084-1090.

[20] Weigl, L.G.; Schreibmayer, W. G protein-gated inwardly rectifying potassium channels are targets for volatile anesthetics. *Mol. Pharmacol.*, **2001**, *60*, 282-289.

[21] keda, K.; Yoshii, M.; Sora, I.; Kobayashi, T. Opioid receptor coupling to GIRK channels. *In vitro* studies using a *Xenopus* oocyte expression system and *in vivo* studies on *weaver* mutant mice. *Methods. Mol. Med.*, **2003**, *84*, 53-64.

[22] Kobayashi, T.; Washiyama, K.; Ikeda, K. Inhibition of G protein-activated inwardly rectifying K^+ channels by fluoxetine (Prozac). *Br. J. Pharmacol.*, **2003**, *138*, 1119-1128.

Received: October 01, 2009 Revised: April 17, 2010 Accepted: May 26, 2010

MOP Reduction During Long-Term Methamphetamine Withdrawal was Restored by Chronic Post-Treatment with Fluoxetine

H. Yamamoto[a,*], Y. Takamatsu[a], K. Imai[b], E. Kamegaya[a], Y. Hagino[a], M. Watanabe[c], T. Yamamoto[a,d], I. Sora[a,e], H. Koga[b] and K. Ikeda[a]

[a]*Division of Psychobiology, Tokyo Institute of Psychiatry, Tokyo, Japan;* [b]*Laboratory for Medical Genomics, Department of Human Genome Technology, Kazusa DNA Research Institute, Chiba, Japan;* [c]*Department of Anatomy, Hokkaido University School of Medicine, Sapporo, Japan;* [d]*Molecular Recognition, Yokohama City University, Yokohama, Japan;* [e]*Department of Psychobiology, Tohoku University, School of Medicine, Sendai, Japan*

Abstract: Previously, we found fluoxetine reduces methamphetamine preference in mice. However, effects of fluoxetine on developed methamphetamine preference and on methamphetamine induced gene expression changes have been largely unknown. The present study investigates effects of post-treatment with fluoxetine on methamphetamine dependence and on gene expressions after long-term withdrawal in mice. First, we examined whether chronic post-treatment with fluoxetine attenuated methamphetamine-conditioned place preference. Next, we examined the changes in gene expression levels after long-term withdrawal (with saline or fluoxetine treatment) following chronic methamphetamine treatment. Using mRNA from the pooled frontal cortices of 10 mice per group, gene expression analyses were performed using a custom-developed cDNA array and a real-time quantitative reverse transcription-PCR. Chronic post-treatments with fluoxetine abolished the conditioned place preference developed by methamphetamine administrations. Even after long-term withdrawal from repeated methamphetamine administration, μ-opioid receptor (MOP) gene expression was significantly reduced in the frontal cortex. The reduced MOP gene expression in the frontal cortex was restored by chronic administration with fluoxetine. These changes were confirmed by Western blot analyses. These findings suggest that the chronic post-treatments with fluoxetine might be effective for restoring the reduction of MOP levels in the frontal cortex following long-term abstinence from methamphetamine.

Keywords: Methamphetamine, conditioned place preference, gene expression, withdrawal, fluoxetine, mu-opioid receptor, frontal cortex, mice.

INTRODUCTION

The development process of sensitization to the behavioral effects of psychostimulants is well-researched. There is substantial evidence that the mesocorticolimbic dopamine system and its excitatory glutamatergic inputs are critical [1, 2]. However, glutamate antagonists do not block the expression of sensitization [3]. Similarly, dopamine antagonists can block the development of sensitization to psychostimulants without blocking its expression [4]. On the other hand, glutamatergic afferents from the prefrontal cortex to the ventral tegmental area and the nucleus accumbens have been reportedly implicated in both the development and expression of sensitization to cocaine and amphetamine [5]. The frontal cortex is important region that is activated in addicted subjects during intoxication, craving, and bingeing, and deactivated during withdrawal [6].

Currently, effective pharmacotherapy for psychostimulant abuse has not been established. However, preclinical studies have indicated that the serotonergic system can effectively modulate the behavioral effects of amphetamine. That is, a negative relationship was observed between the potencies of several cocaine- and amphetamine-like drugs in self-administration studies and their binding affinities for serotonin uptake sites [7, 8]. Administration of the serotonin uptake inhibitor fluoxetine decreased self administration of amphetamine [9] in rodents. Amphetamine withdrawal elevates brain reward threshold in rats [10]. Harrison *et al.* (2001) [11] have reported that co-administration of a 5-HT_{1A} receptor antagonist and fluoxetine reverses reward deficits observed during nicotine or amphetamine withdrawal. These findings suggest that increasing brain serotonin activity can attenuate the behavioral and reinforcing effects of amphetamines.

In the present study, we used the frontal cortices of chronically methamphetamine-injected mice to explore molecules that expressions were changed during long-term abstinence and fluoxetine reversed its expressional changes. First, we applied comprehensive approach to exploration of candidate genes by using cDNA array system utilizing mouse KIAA-homologous cDNA (mKIAA) clones. Next, gene expressions and protein expressions were examined by real-time quantitative reverse transcription-polymerase chain reaction (qRT-PCR) experiments and immunoblot analyses, respectively.

*Address correspondence to this author at the Division of Psychobiology, Tokyo Institute of Psychiatry, 2-1-8 Kamikitazawa, Setagaya-ku, Tokyo 156-8585, Japan; Tel: +81-3-3304-5701; Fax: +81-3-3329-8035; E-mail: yamamoto-hd@igakuken.or.jp

1570-159X/11 $58.00+.00

MATERIALS AND METHODS

Animals

Ten-week-old male C57BL/6J mice were purchased from CLEA Japan (Tokyo, Japan). The experimental procedures and housing conditions were approved by the Tokyo Institute of Psychiatry Institutional Animal Care and Use Committee, and all animals were cared for and treated humanely in accordance with our institutional guidelines on animal experimentation.

Conditioned Place Preference Test

The conditioned place preference test was performed according to the method of Hoffman and Beninger (1988) [12] with some modifications. For this test, we used a two-compartment Plexiglas chamber (Neuroscience Inc., Osaka, Japan). We selected a counterbalanced protocol to nullify each mouse's initial compartment preference [13].

Acquisition of methamphetamine-induce place preference was shown in drug-naive mice. On Day 1, the mice (n = 18 - 20 per group) were allowed to freely explore the two compartments for 15 min. On Day 2, the same trial was performed, and the time spent in each compartment and shuttle numbers were measured for 15 min. Conditioning was conducted once daily for four consecutive days (Days 5-8). Mice were intraperitoneally (i.p.) injected with methamphetamine (2 mg/kg) and immediately confined to the black or white compartment for 50 min on Day 5. On Day 6, the mice were injected with saline and immediately confined to the opposite compartment for 50 min. On Days 7 and 8, the same conditioning as on Days 5 and 6 was repeated. After methamphetamine conditioning, the mice received saline or fluoxetine (20 mg/kg, i.p.) once a day for 10 days (Days 9–18). On the last day (Day 19), the mice were not treated with saline or fluoxetine. The time spent in each compartment and shuttle numbers were measured for 15 min without methamphetamine injection. Time spent in the drug-paired compartment during pre- and post-conditioning preference tests were analyzed by within-group paired t-tests.

Tissue Preparation, RNA Isolation, Probe Labeling, and Microarray Hybridization

For analysis of gene expression studies, mice in the long-term withdrawal groups were given a saline or methamphetamine injection (2 mg/kg, i.p.) once a day for 14 days, housed for 7 days without any injection, and then injected with saline or fluoxetine (20 mg/kg, i.p.) once a day for 14 days and sacrificed 24 h after the last injection.

After decapitation, the frontal cortices from 10 mice per treatment group were quickly dissected on ice, immediately frozen at -80°C, and used as a pooled sample for the cDNA array experiment [14], qRT-PCR analysis and used as separate samples for western blot analysis.

qRT-PCR

To confirm the cDNA array results, qRT-PCR was performed on the MOP gene using the TaqMan strategy (Mm01188089 m1) and the ABI Prism 7300 Sequence Detection System (Applied Biosystems, Foster City, CA). For the expression of the genes other than the MOP gene, real-time qRT-PCR was performed using a cybergreen fluorescence-based assay kit (SBYR Green RT-PCR kit; Takara Bio Inc., Shiga, Japan) according to the manufacturer's instructions. The levels of all cDNAs generated from mRNA by reverse transcription were calculated by the standard curve method for quantification and normalized with respect to GAPDH transcript levels.

Western Blotting

P_2 membranes were prepared from homogenate derived from each frontal cortex. Samples were mixed with an equal volume of Laemmli's samples buffer (10 μg/lane), boiled for 3 min and then resolved on a 5-20% gradient SDS polyacrylamide gel electrophoresis. The proteins were electrotransferred onto PVDF membranes in a semi-dry blotter.

We used two rabbit polyclonal antibodies specific for MOP. *N*-terminal-specific antiserum (N-38) was prepared against 1–38 amino acids sequences of the MOP *N*-terminus [15]. The *C*-terminus-specific antibody (AB5511, lot No. 25050663) was purchased from Chemicon International (Temecula, CA, USA). Rabbit polyclonal anti-actin antibody was purchased from Sigma-Aldrich (St. Louis, MO, USA) and used to detect endogenous actin as an internal standard.

Statistical Analysis

Parametric analysis of quantitative data was performed using a one-way analysis of variance (ANOVA) followed by Scheffe's test. Nonparametric analysis was conducted using the Kruskal-Wallis test followed by Scheffe's *post hoc* comparison test. The level of statistical significance was set at $p < 0.05$.

RESULTS

Effects of Chronic Administration of Fluoxetine on Methamphetamine-Induced Conditioned Place Preference

Time spent in the conditioned compartment was significantly increased when saline was administered for 9 days after methamphetamine conditioning (n = 20, t = 4.408, p = 0.0003; Fig. (**1A**)). By contrast, time spent in the conditioned compartment was not significantly changed when fluoxetine (20 mg/kg) was administered for 9 days after methamphetamine conditioning (n = 18, t = 1.513, p = 0.1488; Fig. (**1B**)). These results suggest that subchronic administration of fluoxetine at a dose of 20 mg/kg to mice weakened the place preference induced by methamphetamine. Thus next, we used mice chronically treated with fluoxetine (20 mg/kg) during methamphetamine withdrawal in the gene expression and western blot analyses.

Effects of Fluoxetine on Methamphetamine-Induced Changes in Gene Expression after Long-Term Withdrawal

In the cDNA array experiments, expressions of a few genes, MOP, N-methyl-D-aspartate (NMDA) receptor 2D subunit (NR2D), nociceptin receptor, G protein-activated inwardly rectifying K^+ channels (GIRKs) and inward rectifier K^+ channel Kir2.3 (IRK3), were reduced after 3 weeks withdrawal following chronic methamphetamine treatment (MAP-Saline column in Table **1**). These reductions (< 70 %

reduction in the saline treatment) were recovered in some genes except GIRK1 and GIRK3 when treated with fluoxetine for 2 weeks after the chronic methamphetamine treatment (MAP-Flx in Table 1). The cDNA array experiments were performed in multiple determinations using a set of pooled samples.

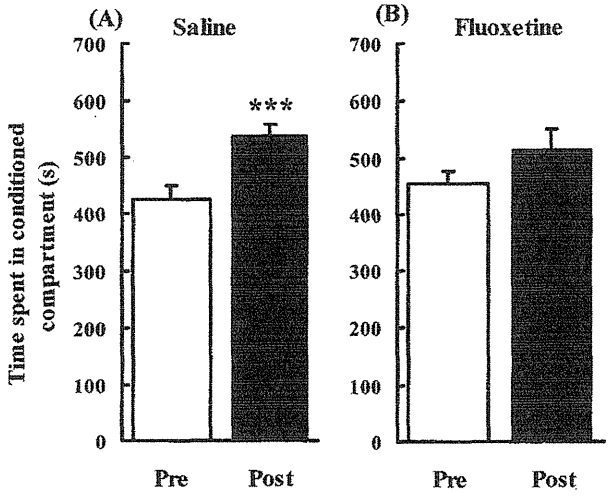

Fig. (1). Effects of chronic administration of fluoxetine on the established methamphetamine-induced conditioned place preference. After methamphetamine conditioning, mice received (**A**) saline or (**B**) fluoxetine for 9 days. Each bar represents mean ± SEM of the time spent in the methamphetamine-paired compartment during a 15-min test session. Pre: preference test during the pre-conditioning phase. Post: preference test during the post-conditioning phase. ***: difference between Pre and Post, $p < 0.001$.

To assess data derived from cDNA array, we performed qRT-PCR analyses on these gene expressions using mRNA derived from three sets of pooled cortices. The qRT-PCR data were shown in parenthesis in Table 1. Expressions of mu-opioid receptor and IRK3 were approximately similar between cDNA array and qRT-PCR analyses. However, gene expressions of NR2D, nociceptin receptor and GIRK2 were not reduced after 3 weeks withdrawal following chronic methamphetamine treatment (parenthesis of MAP-Saline column in Table 1). On the other hand, reduced expression (MAP-Saline) of mu-opioid receptor was recovered by fluoxetine treatment til 93%, while that of IRK3 was 35% (parenthesis of % recovery by fluoxetine treatment in Table 1).

Results using cDNA array experiment and qRT-PCR analyses had shown that the reduced gene expression of MOP in the frontal cortex during long-term withdrawal was restored by subsequent fluoxetine treatments.

Fluoxetine Effects on MOP-Immunoreactivity

To investigate the results obtained from the gene expression analyses, immunoblot of MOP in each frontal cortex of methamphetamine-injected mouse was performed (4 – 12 mice per group). MOP-immunoreactivity (IR) in the frontal cortex was detected as a broad band at a position consistent with a molecular weight of 65,000 with anti-MOP sera (N-38 and AB5511) (Fig. (**2A**)). These two anti-MOP sera (N-38 and AB5511) were specific against MOP molecule. The detected broad bands by these antisera were abolished using MOP knockout mice. MOP-IR with AB5511 antibody of the MAP-Saline sample (3-week withdrawal with saline injections after chronic methamphetamine injections, $n = 11$) was significantly lower than that of the Saline-Saline sample (3-week withdrawal with saline injections after chronic saline injections, $n = 12$) ($p = 0.0101$; Fig. (**2B**)). The intensity of MOP-IR in the MAP-Flx sample (3-week withdrawal with fluoxetine injections after chronic methamphetamine injections, $n = 4$) was significantly higher than that in the MAP-Saline sample ($p = 0.0203$; Fig. (**2B**)) and not different from that in the Saline-Saline sample ($p = 0.902$). The intensity of MOP-IR in the Saline-Flx sample (3-week withdrawal with fluoxetine injections after chronic saline injections, $n = 6$) was not significantly different from those in the Saline-Saline and MAP-Flx samples ($p = 0.699$; $p = 0.473$). These results have shown that MOP-IR was reduced after 3 weeks withdrawal following chronic methamphetamine treatment and this reduction was recovered by subsequent fluoxetine treatments.

DISCUSSION

In the present study, repeated methamphetamine administration induced a conditioned place preference. The place preference was significantly attenuated by chronic fluoxetine treatments during long-term withdrawal. Fluoxetine is reported to reverse reward deficits during amphetamine withdrawal [11]. Recently, Kaneko *et al.* (2007) [16] reported that 5-day treatment with fluoxetine and paroxetine during methamphetamine withdrawal may at least in part reverse methamphetamine-induced behavioral sensitization. Taken together, these results suggest that chronic fluoxetine treatment can partially reverse methamphetamine-induced behavioral changes.

We observed that 3-week withdrawal after chronic methamphetamine induced gene expression changes. Of interest, both in the cDNA array and the real-time qRT-PCR analyses, MOP gene expression was decreased in the frontal cortex after long-term withdrawal, and partially restored by chronic fluoxetine treatment during methamphetamine withdrawal. On the basis of these results of gene expressions, we have performed the protein expressions of MOP by western blot analysis. Of interest, immunoreactive MOP level was significantly reduced during methamphetamine withdrawal, while chronic fluoxetine administrations during withdrawal could partially restore the reduced MOP expression level in the frontal cortex.

To date, changes in MOP expression after withdrawal from alcohol and amphetamine have been reported. Lower MOP binding potential in the right dorsal lateral prefrontal cortex, the right anterior frontal cortex, and the right parietal cortex is associated with higher craving in male alcohol-dependent subjects undergoing alcohol withdrawal [17], even though after long-term abstinence alcoholic patients display no changes in the prefrontal cortex but an increase in the binding potential of MOP in the ventral striatum, including the nucleus accumbens [18]. In contrast, subchronic injections of amphetamine resulted in a significant reduction in MOP mRNA levels in the nucleus accumbens shell [19], whereas no significant changes were observed in the level of

Table 1. Effect of Chronic Fluoxetine Treatment on Changes in Gene Expression After Long-Term Withdrawal Following Chronic Methamphetamine Injections

cDNA Array Result (RT-PCR Result)						
Entrez		Gene(Property)	MAP-Saline	MAP-Flx	Saline-Flx	% of Recovery
Official Symbol	Gene ID			(% of Saline-Saline Control)		by Flx Treatment
		Receptors				
Htr2c	15560	5HTR1C	88.5	78.3	88.9	
Htr1e	107927	5HTR1E	94.8	85.5	107.6	
Htr2a	15558	5HTR2A	108.3	102.6	113.1	
Adra2a	11551	alpha2AR	115.5	93.8	97.5	
Bzrap1	207777	benzodiazapine receptor (peripheral) associated protein 1	88.0	90.0	82.4	
Oprd1	18386	delta-opioid receptor	74.2	90.0	90.0	
Esrrg	26381	estrogen-related receptor gamma	80.4	74.6	83.4	
Oprk1	18387	kappa-opioid receptor	80.4	101.8	115.1	
Lepr	16847	leptin R	95.8	90.7	99.3	
Sigmar1	18391	Sigma-1 receptor	87.9	83.4	96.5	
Oprm1	18390	mu-opioid receptor	58.5 (75.0)	83.4 (98.2)	86.4 (90.1)	60.0 (92.8)
Grm1	14816	mGluR1	105.0	117.5	120.5	
Grm5	108071	mGluR5	84.3	82.6	98.7	
Npy2r	18167	neuropeptideY-Y2 receptor	93.4	93.2	84.5	
Grin2b	14812	NR2B	70.1	78.0	96.1	
Grin2c	14813	NR2C	85.9	79.7	92.3	
Grin2d	14814	NR2D	60.8 (95.3)	64.5 (80.7)	84.2 (88.2)	9.4
Grin1	14810	NR1	88.9	104.8	95.7	
Oprl1	18389	nociceptin receptor	68.8 (102)	91.1 (92.2)	81.5 (92.4)	71.6
Ogfr	72075	opioid growth factor receptor	94.2	105.9	112.7	
		Ion Channels				
Cacna2d2	56808	calcium channel, voltage-dependent,	86.4	103.2	90.8	
Kcnj3	16519	GIRK1	63.4	54.4	70.9	
Kcnj6	16522	GIRK2	66.1 (92.5)	79.0 (106)	78.7 (98.3)	38.2
Kcnj9	16524	GIRK3	57.5	54.4	71.9	
Kcnj12	16515	IRK2	72.3	102.0	96.1	
Kcnj4	16520	IRK3	63.7 (67.3)	76.4 (78.8)	93.1 (70.8)	34.8
Kcns2	16539	K^+ voltage-gated channel, subfamily S, 2	112.3	123.9	122.9	
Rims3	242662	K^+ channel, subfamily K, member 15 and regulating synaptic membrane exocytosis 3	95.0	95.9	123.6	
Kcnt1	227632	K^+ channel, subfamily T, member 1	83.1	95.8	80.2	
Kcnd2	16508	K^+ voltage-gated channel, Shal-related subfamily	76.3	83.5	97.2	
Scn3b	235281	Na^- channel, voltage-gated, type III, beta	90.5	94.5	99.3	

The qRT-PCR data were shown in parenthesis in Table **1**.

Treatment for 2 weeks with saline followed by two weeks with saline (Saline-Saline); treatment for 2 weeks with methamphetamine followed by 2 weeks with saline (MAP-Saline); treatment for 2 weeks with methamphetamine followed by 2 weeks with fluoxetine (MAP-Flx); and treatment for 2 weeks with saline followed by 2 weeks with fluoxetine (Saline-Flx).

Data are presented as percentages of Saline-Saline group, representing the mean ± SEM of 4-16 determinations of pooled samples.

Percentage of recovery was calculated as follows: (1-[(100-[MAP-Flx]value) / (100-[MAP-Saline]value)]) x 100.

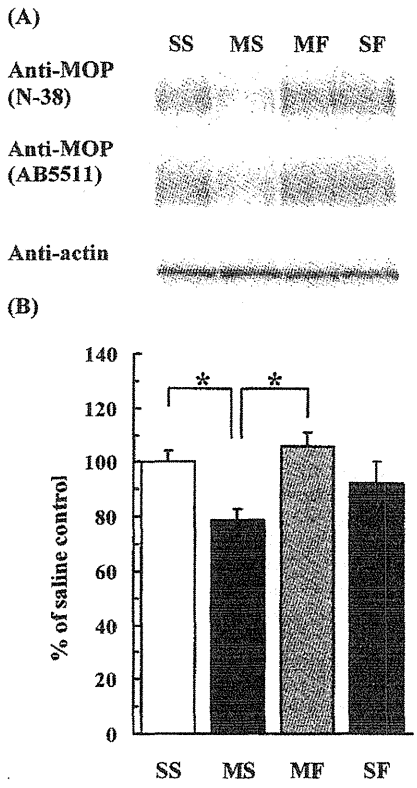

Fig. (2). Immunoblot analyses of changes in MOP protein levels in the frontal cortex by saline or methamphetamine treatment followed by saline or fluoxetine treatment. (**A**) Typical immunoblot with anti-MOP and anti-actin antibodies. Using antiserum selective for MOP *N*-terminal (N-38) or *C*-terminal (AB5511), similar broad bands were detected using the same membrane. Actin levels were measured as references. (**B**) Quantitation of densitometer values using antiserum (AB5511). Values were normalized using actin values and represented as percentage of saline control values. Each bar represents the mean ± SEM of more than four individual mouse frontal cortices. Treatment for 2 weeks with saline followed by two weeks with saline (saline-saline [SS] sample, $n = 12$); treatment for 2 weeks with methamphetamine followed by 2 weeks with saline (methamphetamine-saline [MS] sample, $n = 11$); treatment for 2 weeks with methamphetamine followed by 2 weeks with fluoxetine (methamphetamine-fluoxetine [MF] sample, $n = 4$); and treatment for 2 weeks with saline followed by 2 weeks with fluoxetine (saline-fluoxetine [SF] sample, $n = 6$). *: difference between methamphetamine-saline group and saline-saline group or methamphetamine-fluoxetine group, $p < 0.05$, ANOVA.

MOP mRNA expressed in the nucleus accumbens shell of behaviorally sensitized rats tested 2 or 14 days after withdrawal [20]. Recently, Chiu *et al.* (2006) [21] have used the whole brain except cerebellum repeatedly injected with 2.5 mg/kg of methamphetamine for 7 days and reported that maximal binding of MOP is not changed on days 2 and 5, but down-regulated on day 8. After cessation of drug treatments, the maximal binding of MOP returns to normal level on day 11 and up-regulates on day 21. These data are of interest considering that the expressions of behavioral sensitization were attenuated by pretreatment with 10 or 20 mg/kg of naltrexone either during the induction period or before methamphetamine challenge when they were tested on days 11 and 21 [22]. However they also mention that whole brain samples may be insufficient to reveal the region-specific changes [21]. Investigating methamphetamine-induced craving, endogenous opioid system is involved in the mechanisms underlying cue-induced relapse [23]. Naltrexone inhibits reinstatement of drug-seeking behavior induced by methamphetamine-associated cues, but has no effect on methamphetamine-priming-induced reinstatement. The implication of these results is that there are distinct mechanisms underlying drug-seeking behavior induced by re-exposure to drug-associated cues and that induced by drug priming. Further, the results indicate that increasing activity of the opioid system is involved in the cue-induced drug-seeking behavior, but not in that induced by drug-priming [23]. Naltrexone pretreatment also attenuates context-induced alcohol seeking and inhibits c-fos mRNA expression in the basolateral amygdala and the CA3 subregion of the hippocampus [24]. Therefore, regional specificity is important to study methamphetamine induced behaviors, including conditioned place preference, drug-seeking behavior and behavioral sensitization. To our knowledge, this is the first report of reduced MOP expression in the frontal cortex of long-term methamphetamine withdrawal detected by gene expression and protein expression analyses. This result would provide important insight into the relationship between mu-opioid receptor in the frontal cortex and methamphetamine induced behaviors.

In humans, Ide *et al.* (2006) [25] have shown associations between MOP gene (*OPRM1*) polymorphisms and methamphetamine dependence/psychosis. They also found significant differences in both genotype and allele frequencies of single-nucleotide polymorphisms (SNPs) in the *OPRM1* gene between control and methamphetamine-dependent/psychotic patients. There also is a significant association between SNPs and patients with transient psychosis. These findings suggest that MOP function may affect the development of methamphetamine psychosis. MOP also may be a key molecule involved in the mechanisms underlying behavioral changes after long-term withdrawal following chronic methamphetamine treatment.

In conclusion, the present study showed that reduced mRNA and protein expressions of MOP gene were found in the frontal cortex of methamphetamine-abuse model mice even after long-term abstinence. Furthermore, the subchronic fluoxetine treatment during methamphetamine withdrawal restored MOP expressions. Although the mechanisms underlying the therapeutic effect of fluoxetine for methamphetamine abuse should be further investigated, we suggest a possibility that the restoration of MOP expression can be used as one of therapeutic markers for drug dependence.

ACKNOWLEDGEMENTS

This work was supported by grants from the MEXT (17025054), MHLW (H19-Iyaku-023, H17-Pharmaco-001, H16-Iyaku-029, 18A-3 for Nervous and Mental Disorders), The Naito Foundation, and Foundation for Promotion of Material Science and Technology of Japan (MST). We are grateful to Dr. Makoto Honda for his helpful instruction regarding qRT-PCR analysis and to Dr. Yasukazu Ogai for his excellent advice on statistical analysis.

REFERENCES

[1] Carlezon, W.A., Jr.; Nestler, E.J. Elevated levels of GluR1 in the midbrain: a trigger for sensitization to drugs of abuse? *Trends Neurosci.*, **2002**, *25*, 610-615.

[2] Wolf, M.E.; Sun, X.; Mangiavacchi, S.; Chao, S.Z. Psychomotor stimulants and neuronal plasticity. *Neuropharmacology*, **2004**, *47* (Suppl 1), 61-79.

[3] Wolf, M.E.; Jeziorski, M. Coadministration of MK-801 with amphetamine, cocaine or morphine prevents rather than transiently masks the development of behavioral sensitization. *Brain Res.*, **1993**, *613*, 291-294.

[4] Weiss, S.R.; Post, R.M.; Pert, A.; Woodward, R.; Murman, D. Context-dependent cocaine sensitization: differential effect of haloperidol on development versus expression. *Pharmacol. Biochem. Behav.*, **1989**, *34*, 655-661.

[5] Wolf, M.E.; Dahlin, S.L.; Hu, X.T.; Xue, C.J.; White, K. Effects of lesions of prefrontal cortex, amygdala, or fornix on behavioral sensitization to amphetamine: comparison with N-methyl-D-aspartate antagonists. *Neuroscience*, **1995**, *69*, 417-439.

[6] Goldstein, R.Z.; Volkow, N.D. Drug addiction and its underlying neurobiological basis: neuroimaging evidence for the involvement of the frontal cortex. *Am. J. Psychiatry*, **2002**, *159*, 1642-1652.

[7] Ritz, M.C.; Kuhar, M.J. Relationship between self-administration of amphetamine and monoamine receptors in brain: comparison with cocaine. *J. Pharmacol. Exp. Ther.*, **1989**, *248*, 1010-1017.

[8] Ritz, M.C.; Lamb, R.J.; Goldberg, S.R.; Kuhar, M.J. Cocaine receptors on dopamine transporters are related to self-administration of cocaine. *Science*, **1987**, *237*, 1219-1223.

[9] Porrino, L.J.; Ritz, M.C.; Goodman, N.L.; Sharpe, L.G.; Kuhar, M.J.; Goldberg, S.R. Differential effects of the pharmacological manipulation of serotonin systems on cocaine and amphetamine self-administration in rats. *Life Sci.*, **1989**, *45*, 1529-1535.

[10] Cryan, J.F.; Hoyer, D.; Markou, A. Withdrawal from chronic amphetamine induces depressive-like behavioral effects in rodents. *Biol. Psychiatry*, **2003**, *54*, 49-58.

[11] Harrison, A.A.; Liem, Y.T.; Markou, A. Fluoxetine combined with a serotonin-1A receptor antagonist reversed reward deficits observed during nicotine and amphetamine withdrawal in rats. *Neuropsychopharmacology*, **2001**, *25*, 55-71.

[12] Hoffman, D.C.; Beninger, R.J. Selective D1 and D2 dopamine agonists produce opposing effects in place conditioning but not in conditioned taste aversion learning. *Pharmacol. Biochem. Behav.*, **1988**, *31*, 1-8.

[13] Ide, S.; Minami, M.; Satoh, M.; Uhl, G.R.; Sora, I.; Ikeda, K. Buprenorphine antinociception is abolished, but naloxone-sensitive reward is retained, in mu-opioid receptor knockout mice. *Neuropsychopharmacology*, **2004**, *29*, 1656-1663.

[14] Yamamoto, H.; Imai, K.; Takamatsu, Y.; Kamegaya, E.; Kishida, M.; Hagino, Y.; Hara, Y.; Shimada, K.; Yamamoto, T.; Sora, I.; Koga, H.; Ikeda, K. Methamphetamine modulation of gene expression in the brain: analysis using customized cDNA microarray system with the mouse homologues of KIAA genes. *Brain Res. Mol. Brain Res.*, **2005**, *137*, 40-46.

[15] Kasai, S.; Yamamoto, H.; Kamegaya, E.; Uhl, G.R.; Sora, I.; Watanabe, M.; Ikeda, K. Mu-opioid peptide receptors (MOPS) are detected as broad bands around 65 kDa in western blotting: analyses using MOP knockout mice. *Curr. Neuropharmacol.*, ***in press.***

[16] Kaneko, Y.; Kashiwa, A.; Ito, T.; Ishii, S.; Umino, A.; Nishikawa, T. Selective serotonin reuptake inhibitors, fluoxetine and paroxetine, attenuate the expression of the established behavioral sensitization induced by methamphetamine. *Neuropsychopharmacology*, **2007**, *32*, 658-664.

[17] Bencherif, B.; Wand, G.S.; McCaul, M.E.; Kim, Y.K.; Ilgin, N.; Dannals, R.F.; Frost, J.J. Mu-opioid receptor binding measured by [^{11}C]carfentanil positron emission tomography is related to craving and mood in alcohol dependence. *Biol. Psychiatry*, **2004**, *55*, 255-262.

[18] Heinz, A.; Reimold, M.; Wrase, J.; Hermann, D.; Croissant, B.; Mundle, G.; Dohmen, B.M.; Braus, D.F.; Schumann, G.; Machulla, H.J.; Bares, R.; Mann, K. Correlation of stable elevations in striatal mu-opioid receptor availability in detoxified alcoholic patients with alcohol craving: a positron emission tomography study using carbon 11-labeled carfentanil. *Arch. Gen. Psychiatry*, **2005**, *62*, 57-64.

[19] Vecchiola, A.; Collyer, P.; Figueroa, R.; Labarca, R.; Bustos, G.; Magendzo, K. Differential regulation of mu-opioid receptor mRNA in the nucleus accumbens shell and core accompanying amphetamine behavioral sensitization. *Brain Res. Mol. Brain Res.*, **1999**, *69*, 1-9.

[20] Magendzo, K.; Bustos, G. Expression of amphetamine-induced behavioral sensitization after short- and long-term withdrawal periods: participation of mu- and delta-opioid receptors. *Neuropsychopharmacology*, **2003**, *28*, 468-477.

[21] Chiu, C.T.; Ma, T.; Ho, I.K. Methamphetamine-induced behavioral sensitization in mice: alterations in mu-opioid receptor. *J. Biomed. Sci.*, **2006**, *13*, 797-811.

[22] Chiu, C.T.; Ma, T.; Ho, I.K. Attenuation of methamphetamine-induced behavioral sensitization in mice by systemic administration of naltrexone. *Brain Res. Bull.*, **2005**, *67*, 100-109.

[23] Anggadiredja, K.; Sakimura, K.; Hiranita, T.; Yamamoto, T. Naltrexone attenuates cue- but not drug-induced methamphetamine seeking: a possible mechanism for the dissociation of primary and secondary reward. *Brain Res.*, **2004**, *1021*, 272-276.

[24] Marinelli, P.W.; Funk, D.; Juzytsch, W.; Li, Z.; Le, A.D. Effects of opioid receptor blockade on the renewal of alcohol seeking induced by context: relationship to c-fos mRNA expression. *Eur. J. Neurosci.*, **2007**, *26*, 2815-2823.

[25] Ide, S.; Kobayashi, H.; Ujike, H.; Ozaki, N.; Sekine, Y.; Inada, T.; Harano, M.; Komiyama, T.; Yamada, M.; Iyo, M.; Iwata, N.; Tanaka, K.; Shen, H.; Iwahashi, K.; Itokawa, M.; Minami, M.; Satoh, M.; Ikeda, K.; Sora, I. Linkage disequilibrium and association with methamphetamine dependence/psychosis of mu-opioid receptor gene polymorphisms. *Pharmacogenomics J.*, **2006**, *6*, 179-188.

Received: October 01, 2009 Revised: April 17, 2010 Accepted: May 26, 2010

Psychiatry Research 187 (2011) 312–313

Contents lists available at ScienceDirect

Psychiatry Research

journal homepage: www.elsevier.com/locate/psychres

Letter to the editor

Association study on catechol-*O*-methyltransferase (*COMT*) Val158Met gene polymorphism and NEO-FFI

The *COMT* Val158Met gene polymorphism (rs4680) is associated with psychiatric diseases; the Val allele is associated with higher enzymatic activity than the Met allele (Lotta et al., 1995; Lachman et al., 1996), and it may be related to personality traits.

Association studies on the Val158Met polymorphism and personality traits have been reported, but their results are inconsistent (Eley et al., 2003; Stein et al., 2005; Tochigi et al., 2006; Urata et al., 2007).

We attempted to identify the genetic factors affecting personality traits by examining the association between the Val158Met polymorphism and personality traits, using the Neuroticism Extraversion Openness-Five Factor Inventory (NEO-FFI).

This study was approved by the ethics committee of Azabu University. Blood samples were collected from 143 healthy Japanese adults (40 men and 103 women; mean age, 19.9 ± 1.06 years) after obtaining their written informed consent. They were then evaluated using the NEO-FFI. Genotyping was performed using polymerase chain reaction–restriction fragment length polymorphism (PCR-RFLP) (Erdal et al., 2001). We compared the NEO-FFI scores among the genotypes by performing statistical analysis using one-way analysis of covariance (ANCOVA) with age as a covariate, and Bonferroni's multiple comparisons for adjusted mean values were used as *post-hoc* tests. We applied a Bonferroni correction of a factor of 3 because the three multiple tests are the association of Val/Val, Val/Met, and Met/Met with NEO-FFI scores.

The genotype distribution for the entire participant population was in the Hardy–Weinberg equilibrium (χ^2 (1) = 0.056, $P = 0.813$, with Yates' continuity correction). In all the subjects, agreeableness, as measured by the NEO-FFI, was significantly associated with genotypes (F (2, 139) = 3.44; $P = 0.035$). Multiple comparisons showed that the Val/Val genotype had significantly lower scores than the Val/Met genotype ($P = 0.044$); significant differences in agreeableness and consciousness were observed between individuals with and without the Met allele ($F(1, 140) = 6.92$, $P = 0.010$; $F(1, 140) = 4.54$, $P = 0.035$). Separate analysis of each sex showed that agreeableness was associated with genotypes only in males (F (1, 36) = 4.61, $P = 0.016$). Multiple comparisons showed that the Val/Val genotype exhibited lower scores than the Val/Met genotype ($P = 0.014$); a significant difference in agreeableness in males was observed between the individuals with and without the Met allele (F (1, 37) = 9.34, $P = 0.004$). Moreover, conscientiousness was associated with genotypes only in females (F (2, 99) = 3.89, $P = 0.024$); however, multiple comparisons showed no significant differences. Meanwhile, a significant difference in conscientiousness in females was observed between the individuals with and without the Met allele ($F(1, 100) = 7.14$, $P = 0.009$).

We found that the Val158Met polymorphism may be associated with personality traits.

The NEO-FFI scales showed a significant relationship between this polymorphism and TCI were different in males and females; therefore, physiological reactivity induced by a change in dopamine concentration may be different for each sex. Our results suggest that this polymorphism is associated with agreeableness and conscientiousness, and as far as we know, similar results have not yet been reported. Only single gene polymorphisms are significantly associated with personality traits; therefore, this polymorphism may be an important factor affecting personality traits.

Furthermore, association studies between the Val158Met polymorphism and prefrontal cortex (PFC) function have been performed using the Wisconsin card sorting test (WCST) and the n-back task (Egan et al., 2001; Malhotra et al., 2002; Goldberg et al., 2003; Caldu et al., 2007). Egan et al. reported that fewer perseverative errors occurred in the following order: Met/Met>Val/Met>Val/Val (Egan et al., 2001). The change in the PFC function may affect personality traits.

Further detailed studies may be required to examine the gene polymorphisms of other enzymes involved in the metabolic pathway of the dopamine system.

Acknowledgements

This research was partially supported by The Promotion and Mutual Aid Corporation for Private Schools of Japan, Grant-in-Aid for Matching Fund Subsidy for Private Universities.

References

Caldu, X., Vendrell, P., Bartres-Faz, D., Clemente, I., Bargallo, N., Jurado, M.A., Serra-Grabulosa, J.M., Junque, C., 2007. Impact of the COMT Val108/158Met and DAT genotypes on prefrontal function in healthy subjects. Neuroimage 37, 1437–1444.

Egan, M.F., Goldberg, T.E., Kolachana, B.S., Callicott, J.H., Mazzanti, C.M., Straub, R.E., Goldman, D., Weinberger, D.R., 2001. Effect of COMT Val108/158Met genotype on frontal lobe function and risk for schizophrenia. Proceedings of the National Academy of Sciences of the United States of America 98, 6917–6922.

Eley, T.C., Tahir, E., Angleitner, A., Harriss, K., McClay, J., Plomin, R., Riemann, R., Spinath, F., Craig, I., 2003. Association analysis of MAOA and COMT with neuroticism assessed by peers. American Journal of Medical Genetics 120B, 90–96.

Erdal, M.E., Herken, H., Yilmaz, M., Bayazit, Y.A., 2001. Significance of the catechol-O-methyltransferase gene polymorphism in migraine. Brain Research. Molecular Brain Research 94, 193–196.

Goldberg, T.E., Egan, M.F., Gscheidle, T., Coppola, R., Weickert, T., Kolachana, B.S., Goldman, D., Weinberger, D.R., 2003. Executive subprocesses in working memory: relationship to catechol-O-methyltransferase Val158Met genotype and schizophrenia. Archives of General Psychiatry 60, 889–896.

Lachman, H.M., Papolos, D.F., Saito, T., Yu, Y.M., Szumlanski, C.L., Weinshilboum, R.M., 1996. Human catechol-O-methyltransferase pharmocogenetics: description of a functional polymorphism and its potential application to neuropsychiatric disorders. Pharmacogenetics 6, 243–250.

Lotta, T., Vidgren, J., Tilgmann, C., Ulmanen, I., Melen, K., Julkunen, I., Taskinen, J., 1995. Kinetics of human soluble and membrane-bound catechol O-methyltransferase: a revised mechanism and description of the thermolabile variant of the enzyme. Biochemistry 34, 4202–4210.

Malhotra, A.K., Kestler, L.J., Mazzanti, C., Bates, J.A., Goldberg, T., Goldman, D., 2002. A functional polymorphism in the COMT gene and performance on a test of prefrontal cognition. The American Journal of Psychiatry 159, 652–654.

Stein, M.B., Fallin, M.D., Schork, N.J., Gelernter, J., 2005. COMT polymorphisms and anxiety-related personality traits. Neuropsychopharmacology 30, 2092–2102.

Tochigi, M., Otowa, T., Hibino, H., Kato, C., Otani, T., Umekage, T., Utsumi, T., Kato, N., Sasaki, T., 2006. Combined analysis of association between personality traits and three functional polymorphisms in the tyrosine hydroxylase, monoamine oxidase A, and catechol-O-methyltransferase genes. Neuroscience Research 54, 180–185.

0165-1781/$ – see front matter
doi:10.1016/j.psychres.2010.09.015

Urata, T., Takahashi, N., Hakamata, Y., Iijima, Y., Kuwahara, N., Ozaki, N., Ono, Y., Amano, M., Inada, T., 2007. Gene-gene interaction analysis of personality traits in a Japanese population using an electrochemical DNA array chip analysis. Neuroscience Letters 414, 209–212.

Jun Aoki
Laboratory of Neurophysiology, The Graduate School of Environmental Health Sciences, Azabu University, 1-17-71 Fuchinobe, Sagamihara-shi, Kanagawa 229-8501, Japan
Division of Psychobiology, Tokyo Institute of Psychiatry, Setagaya-ku, Tokyo 156-8585, Japan
Department of Neuropsychiatry, Tokyo Women's Medical University, Shinjuku-ku, Tokyo 162-8666, Japan

Kazuhiko Iwahashi
Laboratory of Neurophysiology, The Graduate School of Environmental Health Sciences, Azabu University, 1-17-71 Fuchinobe, Sagamihara-shi, Kanagawa 229-8501, Japan
Division of Psychobiology, Tokyo Institute of Psychiatry, Setagaya-ku, Tokyo 156-8585, Japan
Department of Neuropsychiatry, Tokyo Women's Medical University, Shinjuku-ku, Tokyo 162-8666, Japan
Health Administration Center, Azabu University, 1-17-71 Fuchinobe, Sagamihara-shi, Kanagawa 229-8501, Japan
Corresponding author. Health Administration Center, Azabu University, 1-17-71 Fuchinobe, Sagamihara-shi, Kanagawa 229-8501, Japan.
Tel./fax: +81 42 769 1930.
E-mail address: iwahashi@azabu-u.ac.jp.

Jun Ishigooka
Department of Neuropsychiatry, Tokyo Women's Medical University, Shinjuku-ku, Tokyo 162-8666, Japan

Kazutaka Ikeda
Division of Psychobiology, Tokyo Institute of Psychiatry, Setagaya-ku, Tokyo 156-8585, Japan

20 March 2009